PHOTOCATALYTIC DEGRADATION OF NO_X, VOCS, AND CHLORAMINES BY TIO_2 IMPREGNATED SURFACES

A Thesis
Presented to
The Academic Faculty

by

Eva Land

In Partial Fulfillment
of the Requirements for the Degree
Master of Science in the
School of Civil and Environmental Engineering

Georgia Institute of Technology
August, 2010

PHOTOCATALYTIC DEGRADATION OF NO_X, VOCS,
AND CHLORAMINES BY TIO_2 IMPREGNATED SURFACES

Approved by:

Dr. Michael Bergin
School of Civil and Environmental Engineering
School of Earth and Atmospheric Science
Georgia Institute of Technology

Dr. L. Greg Huey
School of Earth and Atmospheric Science
Georgia Institute of Technology

Dr. James A. Mulholland
School of Civil and Environmental Engineering
Georgia Institute of Technology

Date Approved: July 1, 2010

ACKNOWLEDGEMENTS

I would like to thank Dr. Mike Bergin who is the advisor of this project. He inspired me not only by supplying cutting edge research ideas, but also by proving that a true balance in life is attainable. In addition I would like to express my gratitude to Dr. Huey, who served as an unofficial co-advisor for this project, and offered many enlightened ideas and comments, in addition to providing the space and resources to carry out this research. I would also like to also thank and the Huey Group, especially Dave Tanner and Bob Stickel. They gave me many hours of their time, and a lot of practical help. I appreciate Dr. Mulholland for volunteering to read this thesis. In addition, The TOTO Corporation supported the majority of this project. I would like to thank my parents and Michelle, Josh, and Abby, my siblings, for giving me guidance, and for being enthusiastic about my studies. I would also like to thank my husband, Adam, for his unfaltering support.

TABLE OF CONTENTS

LIST OF TABLES

LIST OF FIGURES

SUMMARY

Experiments were conducted to determine the photocatalytic degradation of three types of gas-phase compounds, NO_X, VOCs, and chloramines, by TiO_2 impregnated tiles. The oxides of nitrogen NO and NO_2 (NO_x) have a variety of negative impacts on human and environmental health ranging from serving as key precursors for the respiratory irritant ozone, to forming nitric acid, which is a primary component of acid rain. A flow tube reactor was designed for the experiments that allowed the UV illumination of the tiles under exposure to both NO and NO_2 concentrations in simulated ambient air. The reactor was also used to assess NO_x degradation for sampled ambient air. In order to determine the influence of photocatalytic reactions at the tile surfaces on nitrogen containing compounds the change in the concentrations of NO, as well as NOx (NO + NO_2) and NO_y (NO_x plus additional nitrogen containing compounds including HONO and HNO_3) were measured under controlled laboratory conditions. For the NO experiments, it was found that after 72 hours the amount of NO_y removed from the air stream passing over the tiles was 40%. For NO_2, the fraction of NO_y removed was initially ~30%, and approached 0% in approximately twelve hours. The deposition velocities (or photocatalytic velocities, PV) were estimated for NO and NO_2 experiments to remove the influence of concentration and specific experimental conditions on the results. In addition, the overall contact time is irrelevant for the calculation of the PV. Only the residence time over the tiles influences this parameter. The residence time is restricted by the flow rate of the gas, the volume of the reactor, and the surface area of the tiles. The PV values for NO and NO_2 were 0.016 cm s^{-1} and 0.0015 cm s^{-1}, respectively. For ambient experiments a decrease in ambient NO_x of ~ 40% was observed over a period of roughly 5 days. The mean PV for NO_x for ambient air was 0.016 cm s^{-1}

and the maximum PV was .038 cm s^{-1}. Overall, the results indicate that laboratory conditions generally simulate the efficiency of removing NO_x by TiO_2 impregnated tiles. It should be pointed out that under specific conditions, particularly near NO_x sources where there is not a great deal of atmospheric mixing, the tiles may have a substantial impact on local ambient NO concentrations (Maggos et al., 2007).

Volatile organic compounds (VOC's) are formed in a variety of indoor environments, and can lead to respiratory problems (US EPA, 2010). The experiments determined the photocatalytic degradation of formaldehyde and methanol, two common VOCs, by TiO_2 impregnated tiles. The same flow tube reactor used for the previous NO_X experiments was used to test a standardized gas-phase concentration of formaldehyde and methanol. The extended UV illumination of the tiles resulted in a 50 % reduction in formaldehyde, and a 68% reduction in methanol. The deposition velocities (or the photocatalytic velocities, PV) were estimated for both VOC's. The PV for formaldehyde was 0.021 cm s^{-1}, and the PV for methanol was 0.026 cm s^{-1}. These PV values are slightly higher than the mean value determined for NO from the previous experiments which was 0.016 cm s^{-1}. The results suggest that the TiO_2 tiles could effectively reduce specific VOC levels in indoor environments.

Chlorination is a widespread form of water disinfection. However, chlorine can produce unwanted disinfection byproducts when chlorine reacts with nitrogen containing compounds or other organics. The reaction of chlorine with ammonia produces one of three chloramines, (mono-, di-, and tri-chloramine). The production of chloramines compounds in indoor areas increases the likelihood of asthma in pool professionals, competitive swimmers, and children that frequently bath in indoor chlorinated swimming pools (Jacobs, 2007; Nemery, 2002; Zwiener, 2007). A modified flow tube reactor in conjunction with a standardized solution of

monochloramine, NH_2Cl, determined the photocatalytic reactions over the TiO_2 tiles and seven concrete samples. The concrete samples included five different concrete types, and contained either 5 % or 15 % TiO_2 by weight. The PV for the tiles was 0.045 cm s^{-1} for the tiles manufactured by TOTO Inc. The highest PV from the concrete samples was 0.054 cm s^{-1}. Overall the commercial tiles were most efficient at reducing NH_2Cl, compared to NO_X and VOC compounds. However, the concrete samples had an even higher PV for NH_2Cl than the tiles. The reason for this is unknown; however, distinct surface characteristics and a higher concentration of TiO_2 in the concrete may have contributed to these findings.

CHAPTER 1

INTRODUCTION

Unknowingly, the average person will both see and taste titanium dioxide (TiO_2) several times throughout the day. One reason for TiO_2's unobtrusive, yet ubiquitous presence is due to its size; it is a nanoparticle. Since its first discovery at the end of the eighteenth century titanium dioxide has enjoyed a wide variety of applications.

As a naturally occurring oxide of titanium, TiO_2 has three forms: rutile, anatase, and brookite. TiO_2 has a high index of refraction which results in its white appearance, and makes it an opaque solid. This characteristic contributes to TiO_2's pervasive use in paints, plastics, papers, inks, foods, medicines, and toothpastes. TiO_2 absorbs UV light and yet remains stable, and nontoxic at ambient temperatures. These properties contribute to TiO_2's broad applications.

The photocatalytic properties of TiO_2 were first discovered forty years ago (Fujishima & Honda , 1972). Photocatalysis occurs in the anatase form of TiO_2. Ultraviolet (UV) light corresponds to the band gap energy of TiO_2. This provides the valence electrons of TiO_2 enough energy to excite to the conduction band of the semiconductor. The UV exposure thereby creates an electron hole. The photocatalytic reaction of TiO_2 photo-generates valance band holes that can oxidize any organic compound. Any absorbed species will degrade by an electron transfer reaction. In an aqueous solution the strong oxidative potential of the positive holes oxidizes water to create a surface absorbed hydroxyl radical. The electron transfer only occurs on the surface of the TiO_2, and the oxygen radicals that form include $\bullet OH$, $HO_2\bullet$, $O\bullet$, and the superoxide ion O^{2-} (Linsebigler et al., 1995).

The photocatalytic capacity of TiO_2 has resulted in an array of new inventions. TiO_2 can convert UV light into energy in the form of hydrogen (Kawai et al., 1984), which could have energy related applications. The generation of hydroxyl radicals can be harnessed to kill bacteria and fungus (Fujishima & Hashimoto, 1996; Chen, 2009). Additionally there is research to construct TiO_2 based photosensitive oxide semiconductors (Norwothy, 2008). TiO_2 on surfaces can result in photo-induced hydrophilic surfaces, which can be used as an anti-fogging coating (Watanabe et al., 1999). Also, it has been incorporated into building materials to reduce airborne pollutants, and decompose water and soil containments (Chong et al., 2010). The oxidative potential of TiO_2 has caused the production of a new generation of self cleaning and contaminant reducing coatings and materials.

This study analyzed the reactions on TiO_2 with nitrogen oxides (NO_x), volatile organic compounds (VOCs), and monochloramine (NH_2Cl). In all of the experiments TiO_2 commercial grade tiles were used to carry out the analysis. In addition, seven concrete samples were studied in the NH_2Cl experiments. (The concrete samples were only used in for the NH_4Cl experiments due to availability.) The tiles would ideally provide an aesthetically pleasing indoor or outdoor surface coating that would concurrently reduce pollutants. Concrete, on the other hand, is the most abundant manmade material. It is used as a structural support, in buildings, roadways, and in numerous other applications. The inclusion of TiO_2 into concrete samples could result in a profusion of pollutant reducing structures.

1.1 NO_X

It has been well established that heterogeneous chemistry takes place on TiO_2 surfaces involving both oxides of nitrogen, NO_X, and volatile organic compounds, VOC's, under ambient

conditions (Devahasdin et al., 2003; Salthammer et al., 2007; Maggos et al., 2007a,b). The radical species that are generated under UV illumination readily react with adsorbed pollutants, such as NO, impacting their ambient concentrations.

Recent work has focused on the reactions that take place between NO_X and TiO_2 with the objective of evaluating the ability of TiO_2 impregnated surfaces to reduce ambient levels of both NO and NO_2. Although the exact mechanism of the reactions is not entirely understood, it is generally believed that NO is sorbed to the tile surface, and subsequently reacts with oxidants being produced by the interaction of ambient air, UV light and TiO_2 to produce HONO. After HONO is produced it can be further oxidized to NO_2 and then HNO_3. After a period of equilibration it has been suggested that the final step to HNO_3 is no longer applicable and most of the NO is converted to NO_2 (Devahasdin et al., 2003) until the surfaces are cleaned with water. In other words TiO_2 surfaces initially remove NO from the gas phase but after a period of time the tiles become saturated with HNO_3 and most of the NO that reacts at the surface is simply converted into NO_2, until surfaces are cleaned with water.

1.2 VOCs

Many everyday products emit volatile organic compounds (VOCs). Building materials, sprays, and solvents release these molecules. Household products that contain organic chemicals generate significant amounts of VOCs. The emissions from these sources accumulate within buildings. This causes higher indoor VOC concentrations compared to outdoor concentrations. Two volatile organic compounds typically found in indoors include formaldehyde and methanol.

Formaldehyde is a common indoor pollutant. Urea-formaldehyde resins, used as an adhesive in wood products, emit the majority of domestic formaldehyde. Pressed wood products

found in residential buildings, such as particle board, contain this resin. In addition to this adhesive, prior to the 1980's, many homes were constructed with urea-formaldehyde foam insulation. Formaldehyde emissions from these products vary, and generally decrease with time. Indoor levels can range from 0.1 ppm to 0.3 ppm (EPA, 2010). Excess exposure to formaldehyde can irritate the eyes, throat, and lungs. Formaldehyde is also classified as a carcinogen

Methanol, or wood alcohol, naturally occurs in wood and volcanic gases. Decaying organic matter can produce methanol. Paint strippers, aerosol spray cans, wall paints, carburetor cleaners and air wind shield products use methanol as an additive (EPA, 2010). Methanol is volatile under standard atmospheric conditions, and hence exists in the gas-phase. The majority of the methanol releases to the environment are to the atmosphere (EPA, 2010). Long term or high exposure to methanol can cause neurological problems and temporary blindness (EPA, 2010). In addition, methanol can contribute to the formation of photochemical smog when it reacts with other VOCs.

Both formaldehyde and methanol readily degrade on TiO_2 surfaces. At room temperature TiO_2 will oxidize formaldehyde gas to CO_2, and formic acid will form as an intermediate (Pearl & Ollis; Noguchi, 1998; Ao, 2004). In addition formaldehyde readily adsorbs to TiO_2 surfaces (Noguchi, 1998). TiO_2 also efficiently oxidizes methanol. The total redox reaction for methanol is:

$$CH_3OH+3/2O_2 \rightarrow CO_2+2H_2O$$

In an aerated system oxygen is reduced to form water while methanol is oxidized to form CO_2 through a series of reactions (Chen, 1999). The photocatalytic reactions that occur when TiO_2 is

exposed to VOCs have been documented; however, this study determined the efficiency of VOC removal of specific TiO_2 tiles. It was hypothesized that these tiles would effectively reduce both formaldehyde and methanol.

1.3 Chloramines

Chlorination is a common form of water disinfection. Chlorination kills pathogenic microbes and helps keep drinking water potable, swimming pools sanitary, and reduces the organic load in wastewater treatment plants. Chlorine is a widespread disinfectant; however, chlorination can produce unwanted byproducts.

Sodium hypochlorite, NaOCl, is inexpensive and readily accessible. NaOCl, or bleach, is a common household product used for disinfection and whitening. NaOCl is easier to handle then Cl_2 gas; however, both are used for water treatment. Depending on the pH, chlorine forms HOCl, $^-$OCl, or Cl^- in water. These three species are referred to as free chlorine. If a sufficient amount of chlorine is added to the solution the free chlorine species will oxidize reducing molecules, but still remain in their active state. However, if an insufficient amount of chlorine is added then the chlorine will combine with the reducing compounds; thereby becoming 'bound'. For example, chlorine may react with ammonia, (NH_3), amino acids, or manufactured organics and/or inorganics. Bound chlorine has compromised disinfection ability. Depending on the compounds present in the water a wide range of chlorinated species can arise (Shang, 2000). Chlorine reacting with ammonia produces one of three chloramines. These include mono- , di-, or tri- chloramine (NH_2Cl, $NHCl_2$, and NCl_3 respectively). The formation of the chloramines depends on the pH and molar ratio of ammonia to chlorine.

There is concern that the formation of these byproducts not only limits the capability of the chlorine in solution, but also produces noxious gases. After chloramines are formed in solution they escape, due to Henry's Law, to the surrounding atmosphere. Several studies have reported an increased likelihood of asthma in indoor pool professionals, competitive swimmers, and children that frequently bath in indoor chlorinated swimming pools (Jacobs, 2007; Nemery, 2002; Zwiener, 2007). These studies correlated the presence of chloramine gas with an increase in asthma.

Of the three chloramines, monochloramine is the most stable. The concentration of NH_2Cl in solution will remain constant for up to 24 hrs. The overall reaction for the production of monochloramine is:

$$NH_3 + HOCl \rightarrow NH_2Cl + H_2O$$

NH_2Cl has the lowest Henry's Law constant of the three chloramines. Henry's Law determines the partial pressure of a dissolved volatile compound at a constant temperature. Every gas has its own Henry's Law constant that when multiplied by the gas's concentration in the solution gives the partial pressure above the liquid. The Henry's Law constant for trichloramine is so high that it is hard to monitor (Holzwarth, *et al.*, 1984). However, NH_2Cl's Henry's Law constant suggests that monochloramine will remain in solution for an extended time period. Overall NH_2Cl is more reactive than the previous sets of compounds; therefore it was hypothesized that the tiles would reduce monochloramine more efficiently.

This thesis summarizes laboratory experiments involving the time-dependant degradation of gas-phase NO and NO_2, VOCs, and NH_2Cl, over TiO_2 impregnated tile surfaces in the presence of ambient air and UV illumination. The overall objective for the first phase of

experiments was to determine the influence of surface reactions that take place on the tiles, and the gas-phase nitrogen mass balance, focusing on NO_x ($NO + NO_2$) and NO_y (NO_x + other nitrogen containing compounds including HNO_3 and HONO). Several experiments were conducted that exposed tiles to constant concentrations of NO and NO_2. The second set of experiments in this report determined the effect that TiO_2 impregnated tiles have on methanol and formaldehyde reduction. The final phase of experiments determined the reduction of NH_2Cl in the gas phase by the same tiles coated with TiO_2, and seven concrete samples containing varying amounts of TiO_2. The objective of the last phase was to determine the influence of the surface reactions on the gas-phase chlorine and nitrogen mass balance. Overall the experiments provide a comprehensive analysis of the photocatalytic ability of specific TiO_2 samples on several environmentally relevant gas-phase compounds.

CHAPTER 2

EXPERIMENTAL METHODS

The experiments in this study used a modified flow tube reactor to test TiO_2 coated tiles and TiO_2 impregnated concrete samples. The approach was designed to be flexible with respect to gas-phase target compounds and TiO_2 surfaces. The analyses were also developed to be independent of gas-phase concentration, and area of the TiO_2 surfaces.

2.1 NO Experiments

The experiments exposed TiO_2 tiles to known amounts of NO or NO_2 gas in a plug-flow quartz reactor cell illuminated with GE 48" 40 watt UV light that supplied ~ 1 mW cm^{-2} to the tile surfaces. The concentrations of NO were measured at the outlet of the flow cell using a NO analyzer manufactured by Air Quality Design. In addition to NO, the concentrations of NO_x (NO +NO_2) were measured using an NO_2 converter cell also manufactured by Air Quality Design upstream of the NO analyzer. The concentrations of NO_y (NO_x + additional nitrogen containing compounds that include HNO_3 and HONO) were determined using an NO_y converter made by Antron that was intermittently placed upstream of the NO analyzer. For a few specific experiments the concentrations of HONO and HNO_3 were measured using a chemical ionization mass spectrometer (CIMS) fabricated at Georgia Tech. A schematic of the flow cell and the general experimental setup is shown in Figure 1.

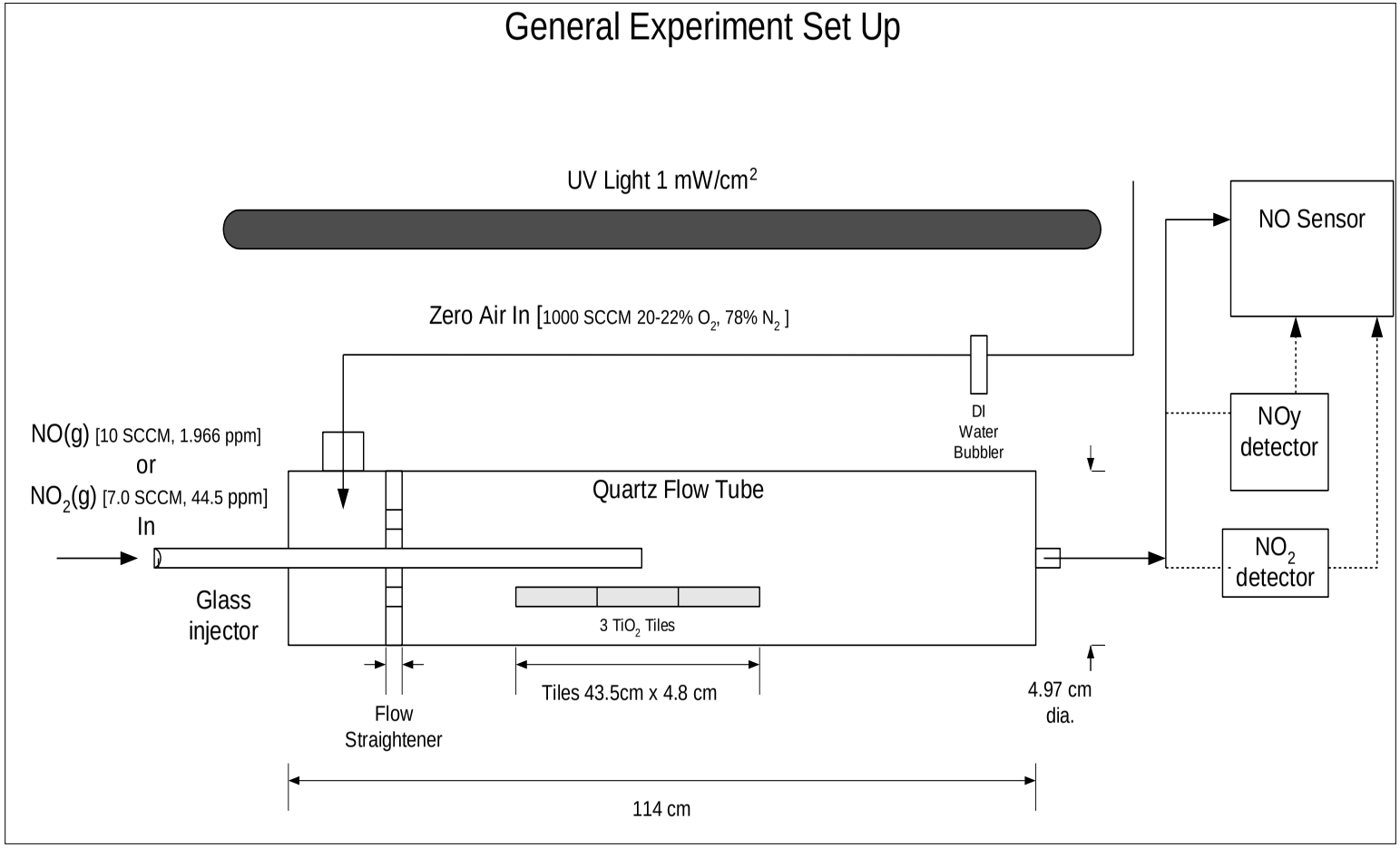

Figure 1: General Experiment Set Up for NO_x Experiments

The flow cell consisted of a quartz tube that was 115 cm long and 4.88 cm inner diameter. Zero air (78 % N_2 and 20-22% O_2) entered the flow cell in a 2 cm diameter quartz port at the inlet end of the flow cell. Prior to entering the cell the zero air passed through a bubbler containing ultrapure deionized water that humidified the zero air. A glass injector tube with an outer diameter 0.65 cm and an inner diameter of .38 cm was used to inject the gas of interest (in this case either NO or NO_2) directly upstream of the tiles. The injector was held in place by an o-ring sealed fitting (Ultra Torr) at the upstream end of the flow cell. This allowed the injector to slide forward or backward changing the amount of surface area exposed to the gas. In addition, near the inlet of the reaction cell a Teflon flow straightener existed to insure that the flow was laminar over the tiles. The zero air, NO, and NO_2 flows were 1000 cm^3 min^{-1}, 10 cm^3 min^{-1} and 7 cm^3 min^{-1} respectively. The flows were maintained using (MKS) mass flow controllers. The concentrations of NO and NO_2 in the standard tanks were 1.996 ppm and 44.5 ppm, respectively. Based on the dilutions with zero air the initial concentration directly upstream of the tile for NO was 19.96 ppb, and NO_2 was 311 ppb for the majority of the experiments. For comparison, typical annual average concentrations of NO and NO_2 in Atlanta measured by the Georgia EPD are 15 ppb and 18 ppb, respectively. Although it should be noted that both NO and NO_2 can have values in the 100's of ppb's depending on the specific atmospheric conditions.

Three TiO_2 impregnated tiles had a total dimension of 4.53 cm *w* x 28.59 cm *l*, and were placed in the flow cell for each experiment. These tiles were provided by TOTO, Inc. The residence time of the mixed zero air and NO/NO_2 gases over the tiles was 215 s. Once out of the quartz chamber the gas traveled through a Teflon tube to the NO sensor. The amount of NO was continuously (1 s sampling frequency) monitored. Depending on the trial the gas could be

diverted to either the NO_2 or NO_y converter before entering the NO sensor. For the trials with NO_2 the gas traveled through the NO_2 converter before entering the NO analyzer.

Generally speaking, the tiles were exposed to NO and NO_2 zero air mixtures over periods ranging from hours to days. Prior to each experiment the tiles and flow cell were extensively cleaned with deionized water. For a given experiment the concentration of the specific target gas was allowed to stabilize before the UV light was turned on. Several experiments were conducted to determine the contribution of reactions occurring on the flow cell walls by removing the tiles at a variety of exposure times, and it was found that wall effects had a negligible influence on the experimental results.

In order to determine the influence of the tiles on NO_x reduction under ambient conditions, outdoor air was also drawn into the sample chamber in a similar manner as described above. NO_x was measured both upstream and downstream of the flow reactor. It should be noted that ambient air contains a wide range of chemical species both in the particulate and gas-phase that may impact the photocatalytic properties of the tiles. Sampling was conducted over a period of roughly five days continuously for the ambient experiment.

2.2 Ultrafine Particle Formation

An additional objective was to determine if ultrafine particles form in ambient air over TiO_2 impregnated surfaces. A Teflon line ran from the roof to the inlet of the flow cell supplying outdoor air. The same tiles and plug-flow reactor that was used in the NO_X experiments were also used in this study. A TSI 3007 Condensation Particle Counter monitored the formation of ultrafine particles at the outlet of the flow cell. The Condensation Particle Counter had a sample flow rate of 100 cm^3 min^{-1}, and measured particles between 0.01 and 1

μm. The tiles were exposed to UV light and ambient air for four twenty minute intervals at various times throughout the day.

2.3 VOCs

The experiments used a Chemical Ionization Mass Spectrometer (CIMS) to analyze the changes in the concentration of formaldehyde and methanol after passing over TiO_2 impregnated tiles. These findings used the same plug-flow setup and tiles as those in the NO_x experiments, described above. However, these experiments include several additional changes. The original design was modified to include a 5.0×10^{-5} aqueous molar solution of formaldehyde. This solution was placed into a glass trap where 50 cm^3 min^{-1} of zero air flowed through the trap, and then mixed with an additional 1000 cm^3 min^{-1} of zero air before entering the flow tube. The mole fraction of formaldehyde in the trap equaled the partial pressure of formaldehyde divided by the total partial pressure. The partial pressure in the trap was calculated using the Henry's Law constant for formaldehyde. To find the partial pressure in the flow tube the trap's partial pressure was multiplied by the flow through the trap and divided by the total flow. The estimated initial concentration of formaldehyde was 780 ppt, or 950 ng m^{-3}.

Once the gas exited the flow tube it entered a proton transfer reaction - mass spectrometer (PTR-MS) (Lindinger, 1993; Hanson et al., 2003). Formaldehyde was detected by the following reaction:

$$CH_2O + H_3O^+ \rightarrow CH_2OH^+ + H_2O$$

Likewise, the reaction for methanol was:

$$CH_3OH + H_3O^+ \rightarrow CH_3OHH^+ + H_2O$$

The protonated formaldehyde, or methanol, then entered the mass spectrometer where it was detected with an ion multiplier. Formaldehyde was detected at 33 (amu or Daltons) and methanol at 31 (amu or Daltons).

Two experiments analyzed the behavior of the TiO_2 tiles. The first experiment recorded only the formaldehyde. In this initial experiment the tiles were illuminated for ten minute intervals. In the second experiment both methanol and formaldehyde concentrations were recorded over six hours of UV illumination.

A third experiment determined the effect that UV intensity has on the reaction. The first two experiments used a GE 48" 40 watt UV light that supplied 1 mW cm^{-2} to the tile surface. In the final experiment a screen was constructed to block 90 % of the light, therefore, illuminating the surface with .1 mw cm^{-2} of UV light. The effect that the decrease UV intensity had on the formaldehyde reactions was then recorded over a two hour period.

2.4 Chloramines

The experiments exposed TiO_2 tiles, and concrete samples containing TiO_2 to a determined amount of monochloramine gas in a plug-flow quartz reactor cell; a modified version of the reactor used in the VOC and NO_X experiments. Two sets of experiments were carried out. The first set exposed the TOTO tiles used in the previous experiments, and the second set exposed seven concrete samples in addition to the commercial tiles to monochloramine gas.

The monochloramine (NH_2Cl) gas was generated from a standardized solution. The gas was prepared by slowly pouring a free chlorine solution over an ammonia chloride solution at chlorine to ammonia molar ratio of 1.2:1 for a two minute period. Prior to mixing both solutions were adjusted to a pH of 10 with sodium hydroxide. The NH_2Cl solution was

prepared in an opaque flask and allowed to stir for an additional 30 minutes. DPD/FAS titration determined the concentration in solution. DPD/FAS titration measures the amount of free chlorine and the combined, (or bound,) chlorine in solution. At a high pH NH_2Cl is the only form of bound chlorine. New standards were prepared daily.

In the first set of experiments two TOTO tiles were exposed to a constant concentration of monochloramine gas. The initial concentration of for NH_2Cl in solution was substantially higher than that found in indoor pools or drinking water. The initial molar concentration was 0.0544 M, or 2.8 g/L. The average concentration reported in pools was .1 mg/L (Li and Blatchly, 2009). The sensitivity of the CIMS required that the concentration over the tiles be much higher than that found in public environments.

The flow cell consisted of a quartz tube that was 28.8 cm long and 4.88 cm in diameter. The solution of NH_2Cl was placed in line before the flow cell. Clean zero air (78 % N_2 and 20-22% O_2) was bubbled through the NH_2Cl solution at 10 cm^3 min^{-1}. This flow was then attached to a T with an addition 200 cm^3 min^{-1} of zero air. The combined flows entered at the flow cell inlet. All of the tubing and fittings were Teflon. The flows were maintained using (MKS) mass flow controllers. The partial pressure above the solution was calculated using Henry's law, (Holzwarth, 1984). To find the gas phase concentration in the flow tube the partial pressure above the solution was multiplied by the gas flow bubbled through the solution flask and divided by the total flow. The estimated initial concentration of monochloramine was 2.43 x 10^6 ug m^{-3}.

Two TiO_2 impregnated tiles had a total dimension of 4.53 cm *w* x 19.06 cm *l*, and were placed in the flow cell for each experiment. The residence time of the zero air and the NH_2Cl gas

over the tiles was 96.6 s. Once out of the quartz chamber the gas traveled through a Teflon tube to the inlet of the CIMS. The reaction that resulted in the PT-RMS front-end of the CIMS was:

$$NH_2Cl + H_3O^+ \rightarrow NH_2ClH^+ + H_2O$$

The amount of chloramine gas was continuously sampled, monitored, and recorded in Hz/ppt. A diagram of the experimental setup is depicted in Figure 2.

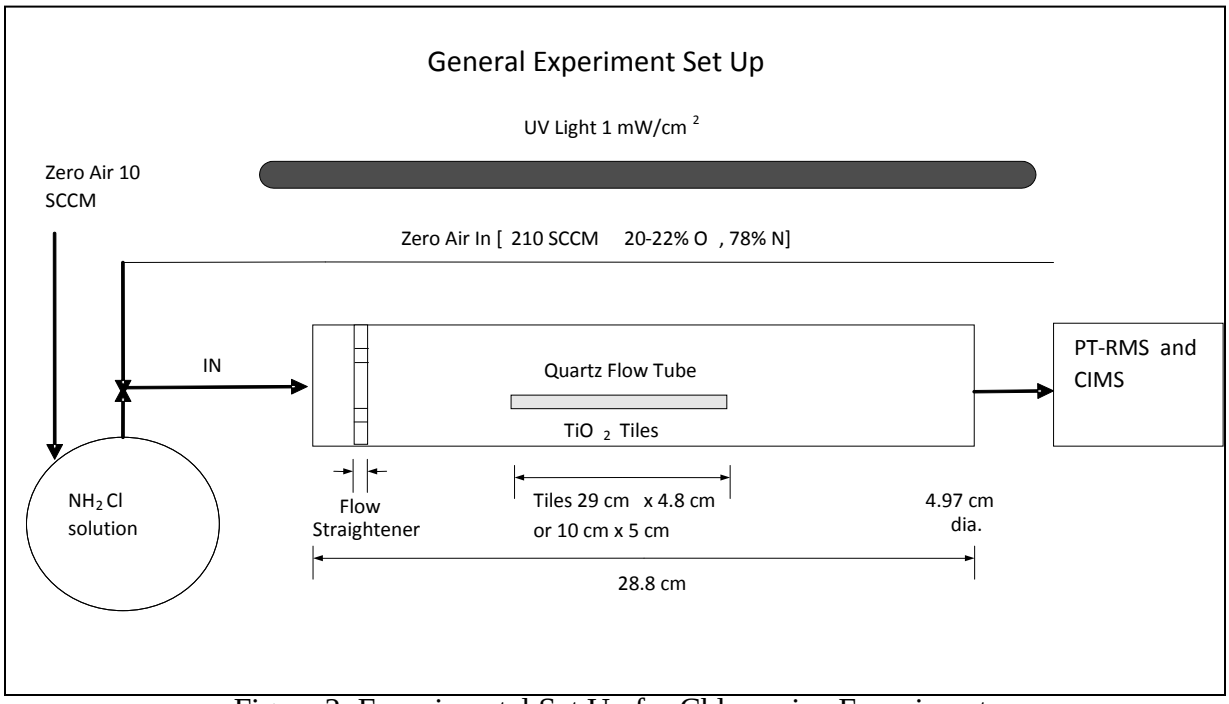

Figure 2: Experimental Set Up for Chloramine Experiments

Two sets of experiments were preformed on the TOTO tiles. The first set exposed the tiles for two 30 minute intervals, and in the second the tiles were illuminated for six hours. Prior to each experiment the tiles and flow cell were extensively cleaned with deionized water. The sensitivity of the CIMS was calibrated, and the concentration reductions are shown in the next section.

In the second round of NH_2Cl experiments both the TOTO tiles and seven sets of concrete tiles were exposed. Of the seven sets, there were five different types of concrete used. Each sample tile had dimensions of 5 cm *w* x 10 cm *l*. The tiles are labeled below as 10-5, (PC10 concrete, 5% TiO_2), 25-5 (P25 concrete, 5% TiO_2), 25-15 (P25 concrete, 15% TiO_2), 50-5 (PC50 concrete, 5% TiO_2), 50-15 (PC50 concrete, 15% TiO_2), 105-5(PC105 concrete, 5% TiO_2), 500-5 (PC500 concrete, 5% TiO_2). The first number corresponds to the type of concrete, and the second to the percentage by weight of TiO_2. Therefore, the samples either contained 5% TiO_2, or 15% TiO_2. The TiO_2 in Samples containing 10, 50,105, and 500 concrete was manufactured by Millennium Chemicals. The TiO_2 in the 25 samples were manufactured by Degussa Chemicals. The concrete samples themselves were manufactured in the Civil Engineering Department of Georgia Tech.

The concrete samples were placed in the same flow tube setup as the earlier NH_2Cl experiment. However, do to the smaller surface area the residence time over the tiles was reduced to 53.43 seconds. For a more accurate comparison between the TOTO tiles and the concrete samples only one TOTO tile was used during these experiments. This was done so that a similar surface area, and therefore a similar residence time would remain consistent between samples. In these experiments the initial concentration was lowered to 8.55×10^4 ug m^{-3} in the gas phase; this corresponds to a molar concentration in solution of 1.94×10^{-3} M. For each of the seven concrete and the TOTO samples both a 30 minute trial and a 3 hour trial was performed.

For both the TOTO and the concrete samples a surface analysis was performed after the 3 hour experiment. The samples were washed with 100mL DI H_2O, and the wash was then

analyzed in an ion chromatograph (IC). The concentrations for the anions on the surface were characterized.

CHAPTER 3

RESULTS AND DISCUSSION

The experiments determined the time-dependant degradation and gas-phase effects for NO_X, VOCs, and chloramines over the TiO_2 impregnated surfaces in the presence of UV illumination. The figures and data below characterized the reduction of the specified compounds. For comparison an equation for the mass deposition, (mass flux), and the photocatalytic velocity was developed. This equation, described further below, allows for a comparison between compounds, concentration, and tiles. The experiments focused on gas-phase reduction, and the overall mass balance.

3.1 NO_X Experiments

The relative concentrations of NO, NO_x, and NO_y are given in Figure 3. All three nitrogen compounds are represented in the graph below as NO_N. It should be noted that all of the results are scaled with respect to the initial NO concentration entering the flow cell. Therefore the 110% initial concentration of NO_y is a result of additional unaccounted for nitrogen species present in the standard gas at the start of the experiment. The initial results indicate that nearly 80% of the NO gas is initially removed from the flow cell for the conditions of our experiments due to reactions taking place on the tile surface. The results also indicate that NO and NO_2 account for nearly all of the total NO_y.

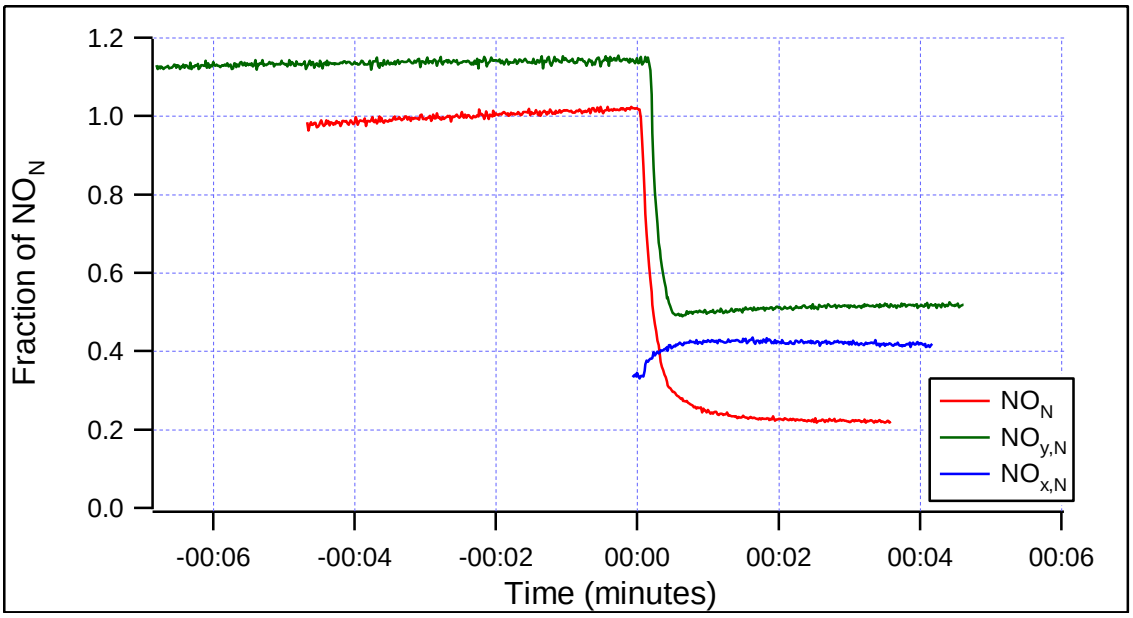

Figure 3: Initial Results for NO Injected into Flow Cell with UV illumination

Figure 4 shows the fraction reduction of NO over a 40 hour period of UV illumination (note that the concentrations are scaled relative to the initial nitrogen volume concentration as NO_y which we denote $NO_{y,N}$). Similar to Figure 3, an initial decrease of roughly 80% is seen for NO that with time is relatively constant. The results indicate a dynamic response of the tiles with respect to the nitrogen balance over the tiles. This is seen by the fact that both the NO_y and NO_x concentrations are at a minimum initially and then increase with time. In fact, the NO_y depletion over the tiles decreases from an initial value of 80% to 60% after 40 hours, with the balance of the output at the end of the experiment being roughly half NO and half NO_2. It is worthwhile to note that at the end of the experiments the HONO concentrations and HNO_3 concentrations were also measured. The HNO_3 concentration was negligible (< 100 ppt) while the HONO concentration was ~ 500 ppt. In general this is further evidence that NO and NO_2 dominate the gas-phase nitrogen budget over the tiles.

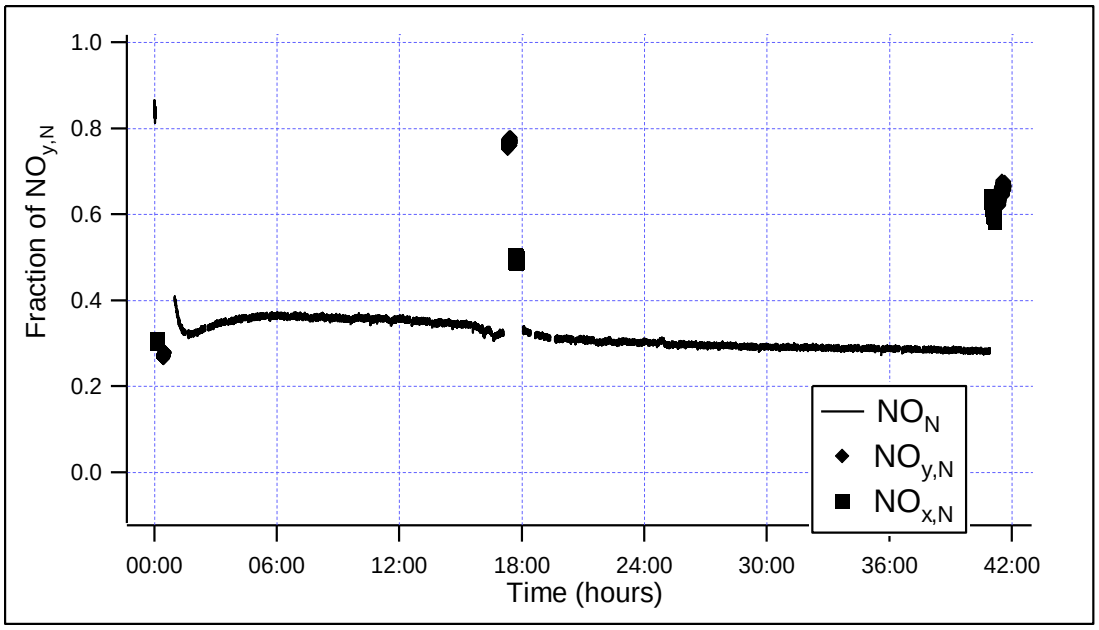

Figure 4: NO Experiments With UV Illumination Over 40 Hours

Several steps were taken to determine the overall mass balance. In one study the tiles were illuminated for 4 hours and then washed with ultrapure deionized water. It was found that 0.0498mg of nitrate (NO_3^-) had deposited on to the tiles surface. Over that time frame 0.295 grams of total nitrogen entered the cell. Therefore approximately 0.17% of the total nitrogen had been converted and deposited onto tiles surface in the form of nitrate (NO_3^-). It should be noted previous research has indicated that initially NO deposited to tiles generates nitrite (NO_2^-) in greater abundance than nitrate (NO_3^-) from nitric acid production. Therefore the results are not surprising given that the unaccounted for nitrogen deposition is likely in the form of nitrite on the surface of the tiles. Unfortunately we did not measure nitrite in our analyses.

For a more complete long term assessment of the nitrogen mass balance NO was injected into the flow cell for 72 hours, with NO_y being measured continuously. At the end of the experiments NO_x and NO were measured. As shown in Figure 5, and consistent with previous results, the initial removal of total NO_y is roughly 80%. The NO_y removal is ~70% after 40 hours

(Figure 5), comparable to ~60% achieved in the previous experiment (Figure 4). After 72 hours the tiles still remove 60% of the total NO_y, and the NO_y is comprised primarily of NO and NO_2.

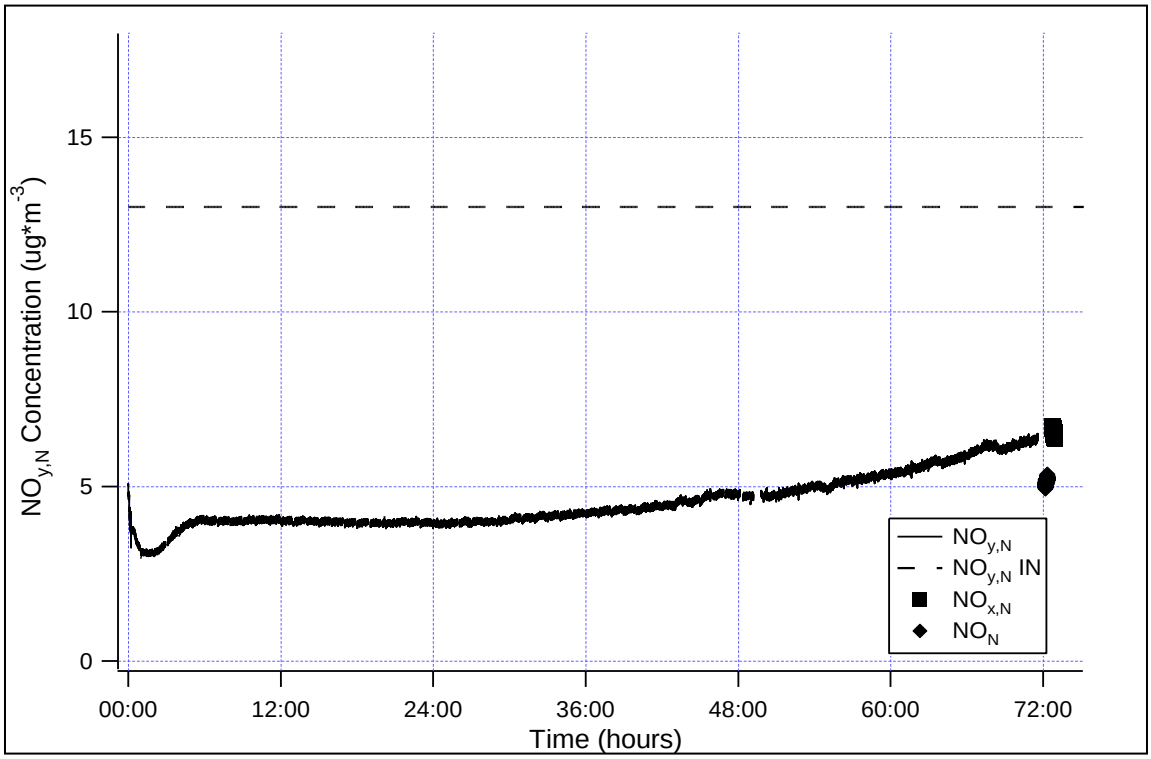

Figure 5: Continuous Measurement of NO_y With NO Injection and UV Illumination

Based on the results shown in Figure 5, the flux of NO_y can be estimated based on a mass balance as follows:

$$F_{NO_y} = \frac{H}{\tau}(C_i - C) \qquad (1)$$

Here F_{NOy} is the NO_y mass flux (μg $m^{-2}s^{-1}$), H is the distance from the top of the flow cell to the surface of the tiles sitting within the flow cell (0.028 m), τ is the residence time of over the tiles (215 s), C_i is the initial concentration of NO_y before it passes over the tiles (μg m^{-3}), and C is the

concentration of NO_y (µg m^{-3}) at the outlet of the flow cell. Figure 6 shows the mass flux of $NO_{y,N}$ (we choose to plot the mass flux of N in part since we do not know all of the chemical constituents that make up the NO_y species and hence cannot estimate the actual NO_y mass flux). As seen in Figure 6, the peak in the mass flux occurs within the first several hours, this point is where the largest difference exists between the initial an outlet concentrations as seen in Figure 5. The flux decreases as the difference in the inlet and outlet concentrations of the flow cell decrease overtime. The results are in general agreement with those of Devahasdin et al. (2003) who found an initial maximum flux related to an initial high rate of chemisorption of NO to a TiO_2 coated surface, followed by a gradual decrease in NO_x degradation as the system goes towards a steady state.

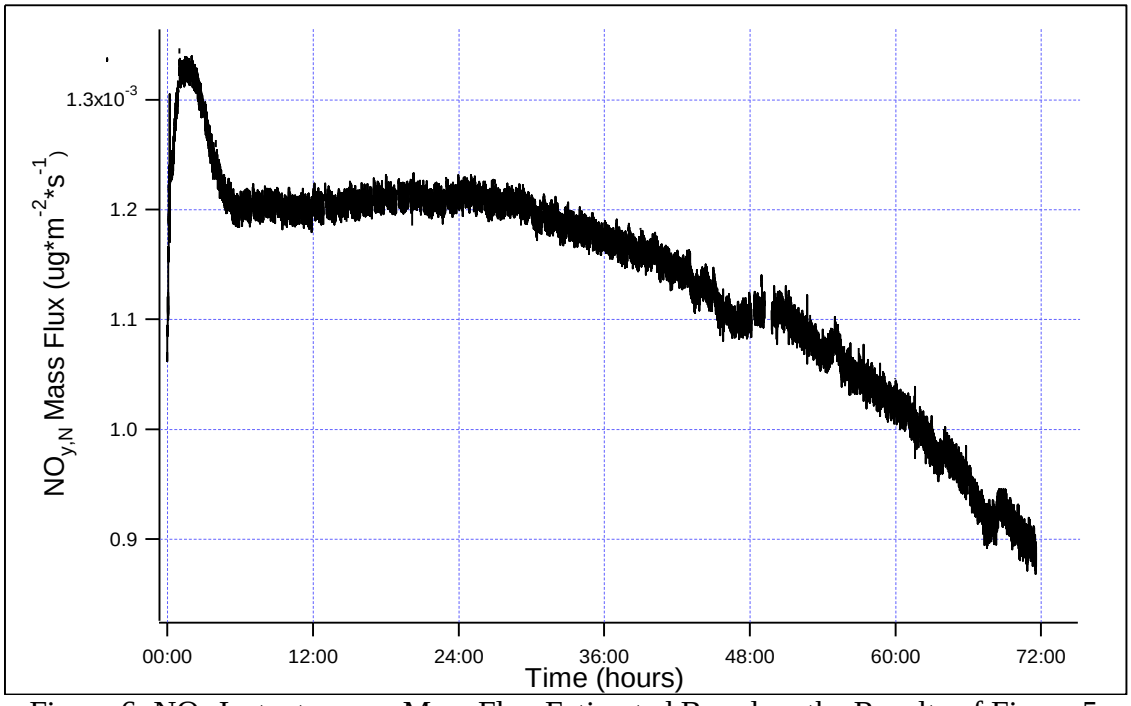

Figure 6: NO_y Instantaneous Mass Flux Estimated Based on the Results of Figure 5

In order to determine the overall influence of tile surface reactions on the NO concentrations in the flow cell, the deposition velocity was estimated. The deposition velocity, which is also called the photocatalytic velocity (PV), is a preferred parameter to compare results for different laboratory methods and is perhaps the most important parameter to use to estimate the removal of NO_x under specific ambient conditions. PV is estimated as the ratio of the flux of the compound of interest divided by the average of the inlet and outlet concentrations. The equation for PV can be written as:

$$PV = \frac{2\ F_{NOy}}{(C_i\ ^{+}\ C)} \qquad (2)$$

The maximum PV of ~0.016 cm s^{-1} for $NO_{y,N}$ occurs at ~ 3 hours (Figure 06). This value is in rough agreement, although at the lower end of values reported for deposition of NO_x to TiO_2 impregnated paint walls (Maggos et al., 2007).

A key feature of Figure 6 is that it can be integrated with time to estimate the total flux of nitrogen mass associated with NO_x and NO_y related compounds. Figure 7 shows the cumulative flux of nitrogen ($NO_{y,N}$) to the tile surface for two separate trials. As shown in the plot, the cumulative deposition over 72 hours is ~ 250 µg m^{-2}). An important feature of the plot is that the slope of the curve is relatively constant suggesting that the tiles are still net sinks for NO after 72 hours. The results for both trials are also very similar. Assuming that under actual ambient conditions precipitation washes the tiles every 3-5 days suggests that the tiles will not become saturated with nitrogen containing compounds in typical outdoor applications.

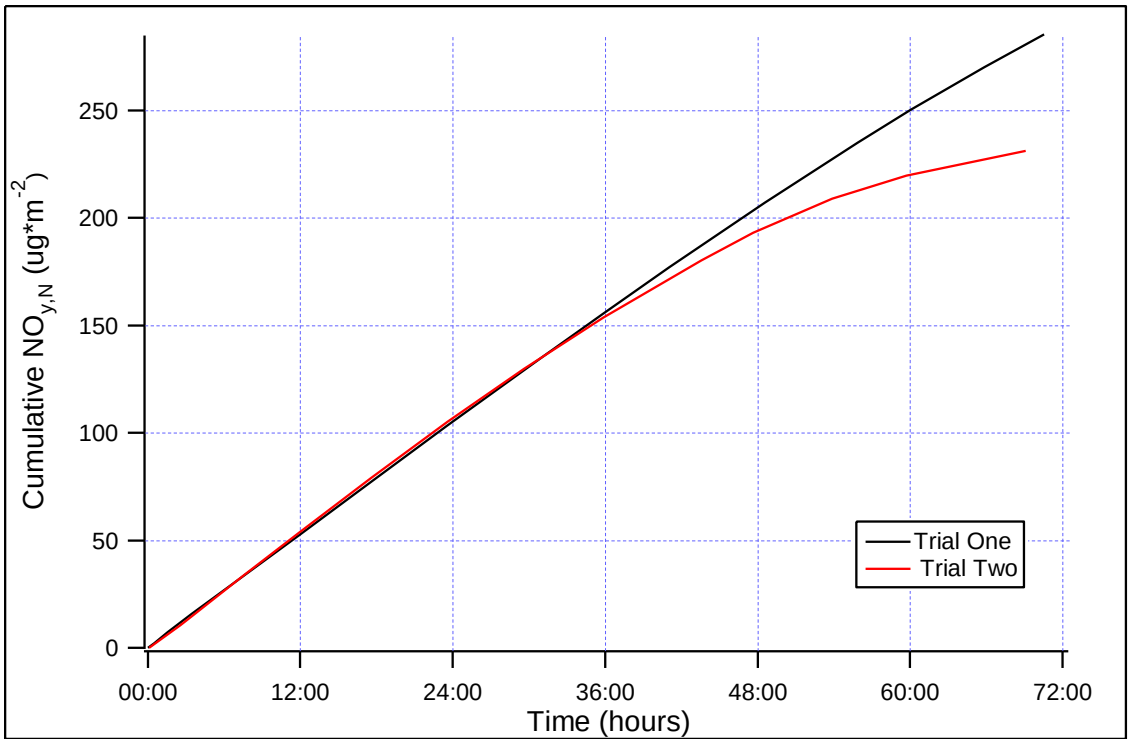

Figure 7: NO_y Cumulative Flux for NO Injection for Two Separate Experiments

3.1.1 NO_2 Experiments

Figure 8 shows the change in both NO_x and NO_y concentrations (normalized to the initial NO_2 concentration) as NO_2 is injected into the flow cell. Similar to NO, there is a substantial initial decrease in the NO_2 concentration (~40%), with an accompanying decrease of ~ 30% NO_y. In general, the result that NO_2 is less influenced by TiO_2 surface reactions is consistent with previous findings (Maggos et al., 2007).

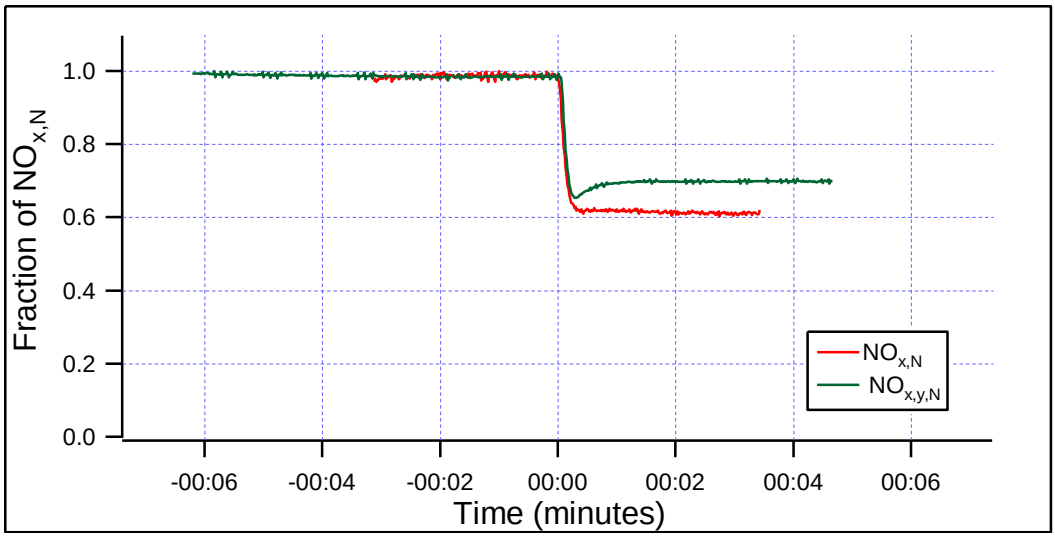

Figure 8: Relative Change in Concentrations for NO_2 Input into Flow Cell

In order to gain insight into the mass balance of NO_x and NO_y in the test gas-streams $NO_{y,N}$ was measured continuously over 24 hours. After roughly 12 hours the difference in the initial concentration of $NO_{Y,N}$ and concentration at the outlet in the flow cell is negligible as shown in Figure 9. As with the NO experiments, NO and NO_2 each accounted for roughly half of the nitrogen compounds in the outlet gas stream. It should be pointed out that the initial concentration of NO_2 (311 ppb) is significantly greater than that of NO for the previous experiments (19.96 ppb) and the increased flux of NO_2 due to the larger concentration gradient resulted in a saturation of the tile surface that did not occur for the NO experiments.

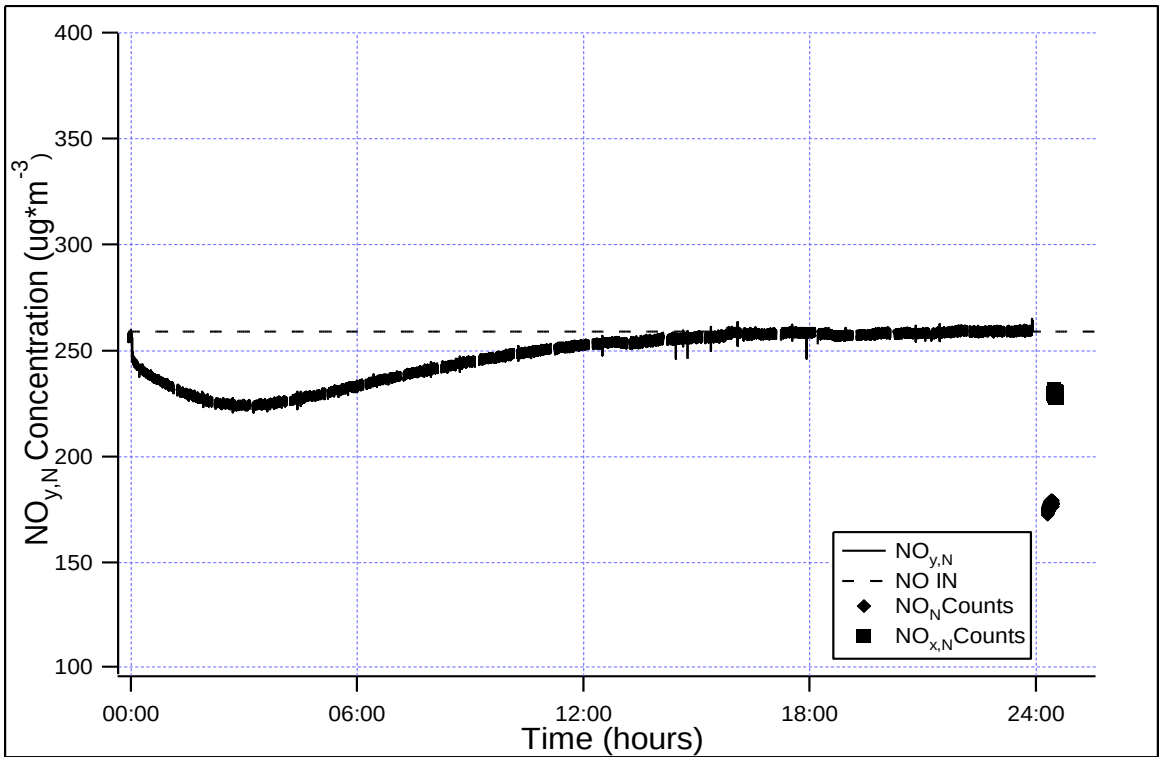

Figure 9: $NO_{,y,N}$ Experiments for NO_2 Input Into Flow cell

In Figure 10 the $NO_{y,N}$ flux is plotted using Equation 1 and the results shown in Figure 08. The mass flux of $NO_{y,N}$ becomes roughly zero at 12 hours due to the fact that the concentration gradient (difference between the initial and outlet concentrations) is negligible after that time. The net PV velocity estimated at the point of maximum flux (~ 4 hours) is 0.0015 cm s^{-1},which is less than the value of 0.016 cm s^{-1} estimated for NO. Although the reason for this is not entirely clear, it is likely due in part to the ability of the tiles to more readily sorb NO versus NO_2. The cumulative $NO_{y,N}$ deposition estimated from Figure 10 is shown in Figure 11. The cumulative flux of 100 µg m^{-2} for NO_2 is roughly a factor of 4 lower than that for NO. It is also clear that the tiles became saturated with respect to NO_2 deposition for the experiments.

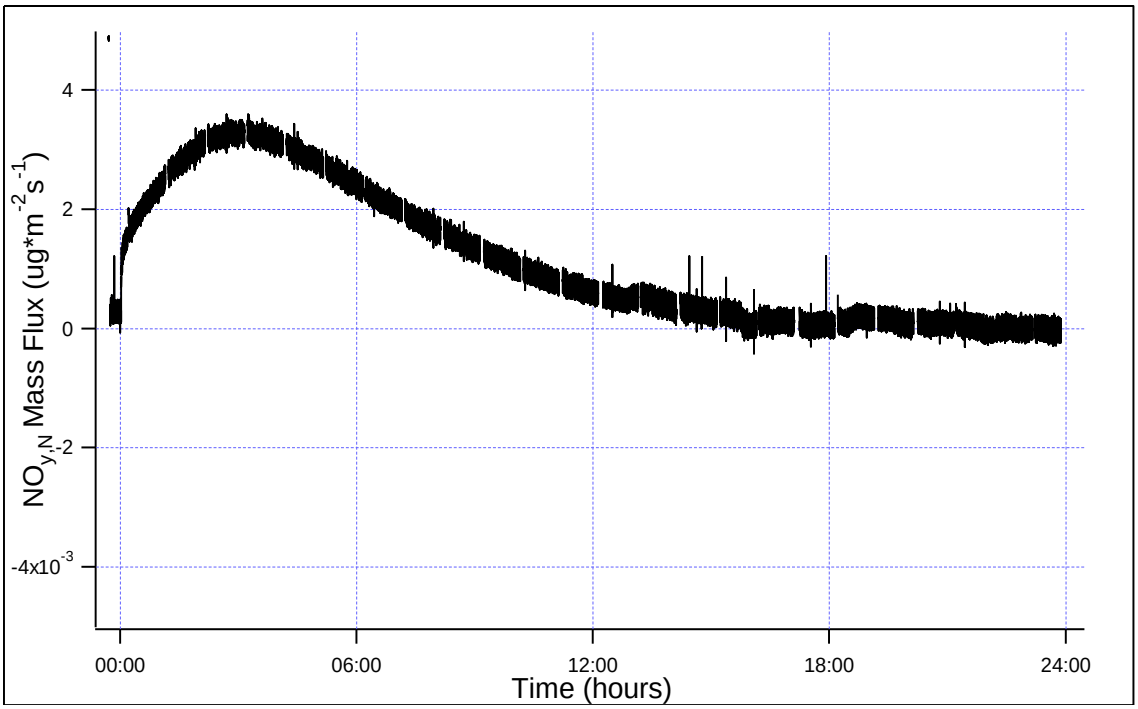

Figure 10: $NO_{y,N}$ Experiment Mass Flux

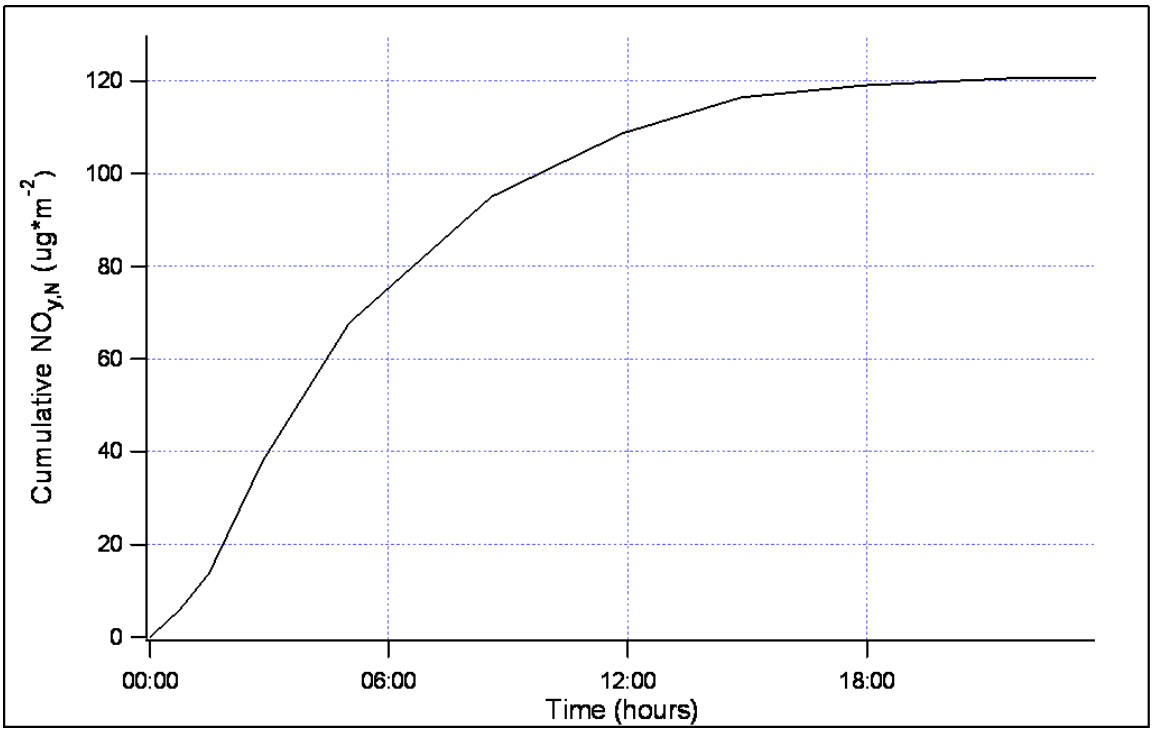

Figure 11: Cumulative $NO_{,y,N}$ Deposition

3.1.2 Outdoor Air Experiments

Figure 12 shows the change in NO_x concentrations upstream and downstream of the flow-through reactor for ambient air. In general NO_x concentrations are highest during morning rush-hour, and lowest in the early afternoon as the atmospheric boundary layer increases and dilutes the surface emissions with relatively clean air from aloft. As shown in Figure 12, the decrease in NO_x due to photocatalytic degradation associated with the tiles is ~40%. The photocatalytic velocity, PV, based on Figure 12 reaches a maximum of 0.038 cm s^{-1}, and averages at .016 cm s^{-1}. The PV values estimated as a function of time for the entire measurement period are shown in Figure 13. This PV value is the same as the PV for the laboratory experiments with NO. It should be noted that over the five day period the tiles continued to degrade ambient NO_x with a somewhat constant PV value, suggesting the tiles did not become ineffective with time. Overall, the ambient results suggest that the tiles are similarly effective at removing NO_x under ambient conditions compared with laboratory conditions with zero air (i.e. relatively pure air) and water vapor.

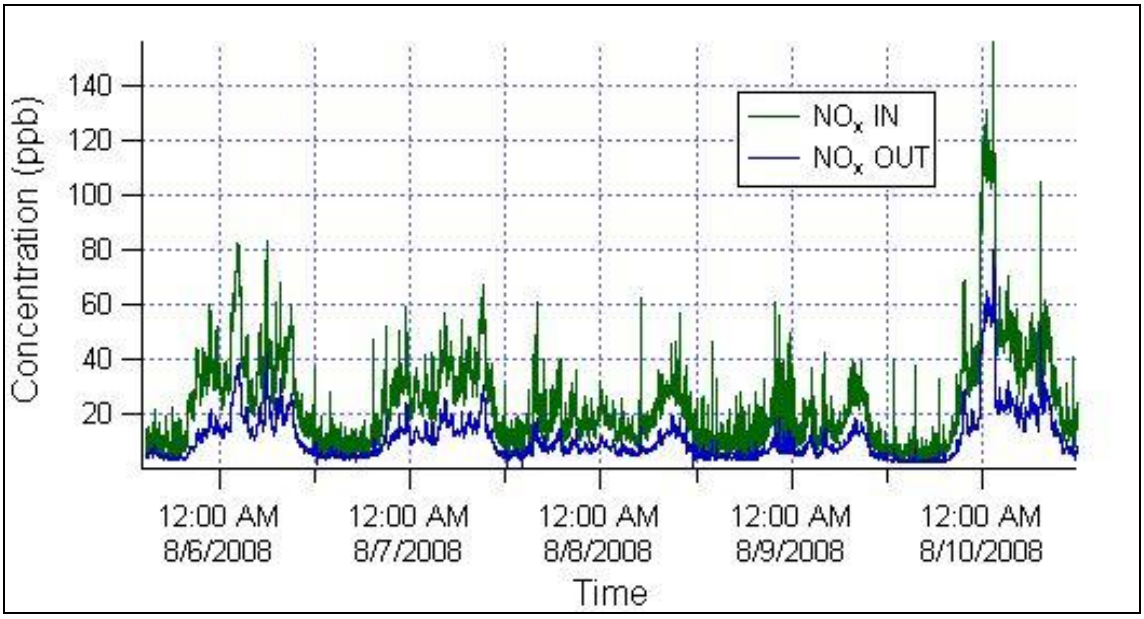

Figure 12: NO_x Concentrations Upstream (NO_x IN) and Downstream (NO_x OUT) of the Flow-Through Reactor

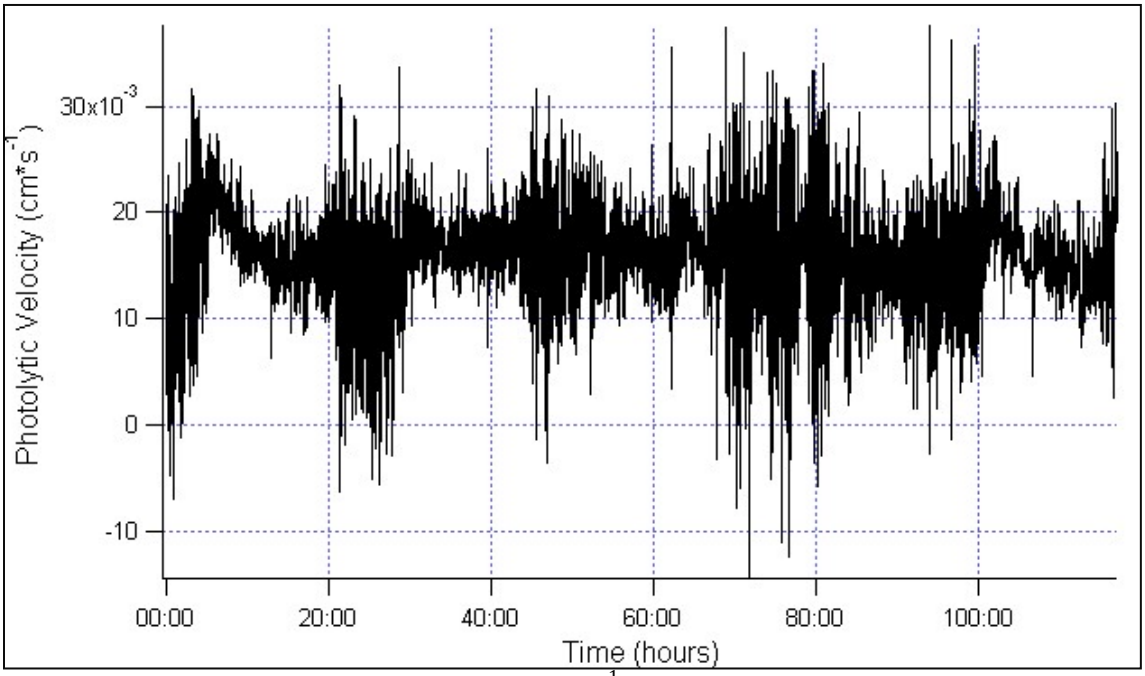

Figure 13: NO_X Photocatalytic Velocity (cm s^{-1}) as a Function of Time for Ambient Air

3.2 VOC Experiments

The concentration and the photolytic velocity for the VOC experiments are depicted in the graphs below. The photocatalytic velocity is dependent on the VOC's mass flux. The equation for the VOC's mass flux was the same as the mass flux equation used for NO_x, Equation 1. Where F_{voc} is the VOC mass flux ($\mu g\ m^{-2}s^{-1}$), H is the distance from the top of the flow cell to the surface of the tiles sitting within the flow cell (0.028 m), τ the residence time of over the tiles (215 s), C_i represents the initial concentration of the VOC before it passes over the tiles ($\mu g\ m^{-3}$), and C the concentration of the VOC ($\mu g\ m^{-3}$) at the outlet of the flow cell. The photocatalytic velocity was determined using the initial concentrations of the formaldehyde and methanol respectively in Equation 2.

In the initial VOC experiment the UV light was on for two, ten minute intervals, as characterized in Figure 14. On this graph the red crosses, superimposed over the concentration, represent the photocatalytic velocity. A maximum reduction of 25% occurred after the light was on for ten minutes. Corresponding to this time the PV reached a minimum of approximately $45x10^{-4}\ cm*s^{-1}$. Figure 14 represents the tiles reduction capacity for a short period of time.

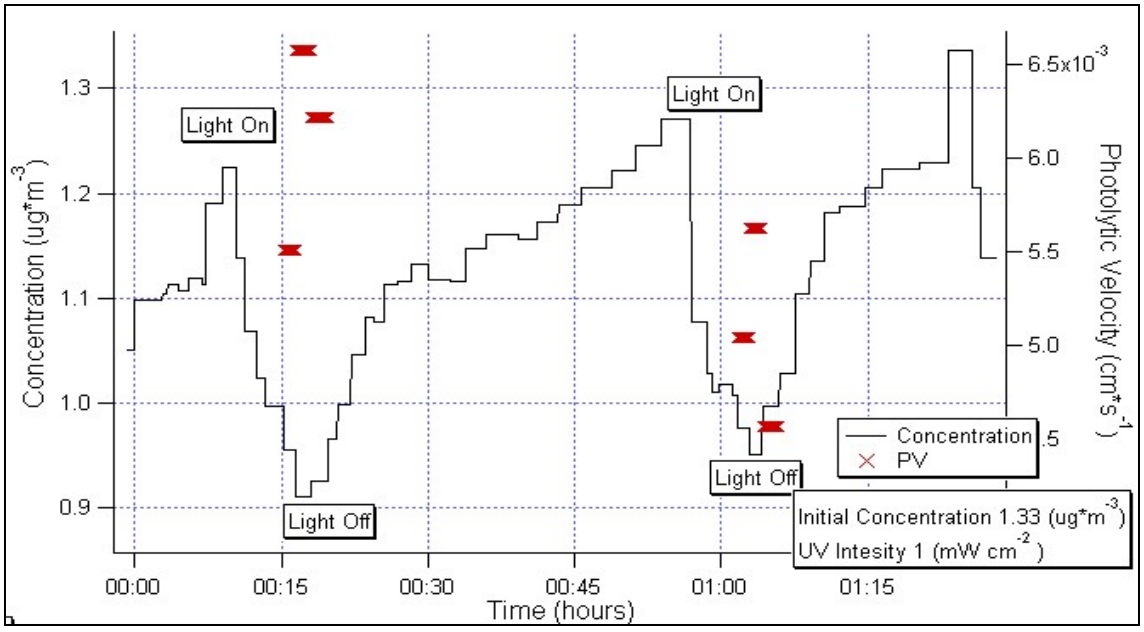

Figure 14: Initial Formaldehyde Reduction and Photocatalytic Velocity

To determine the long-term effects a second experiment was conducted for six hours. Figure 15 shows the concentration of formaldehyde for this duration. The inlet concentration, depicted by the dashed red line, remained at 954 ng m^{-3}. After two hours the outlet concentration stabilized to an average of 455 ng m^{-3}. This corresponds to a 52 % reduction. Figure 15 has an increased amount of noise, and the reason for this remains unclear. However, the values only fluctuate by 20 to 30 %. Therefore, despite the range the tiles still significantly reduce the outlet concentration of formaldehyde.

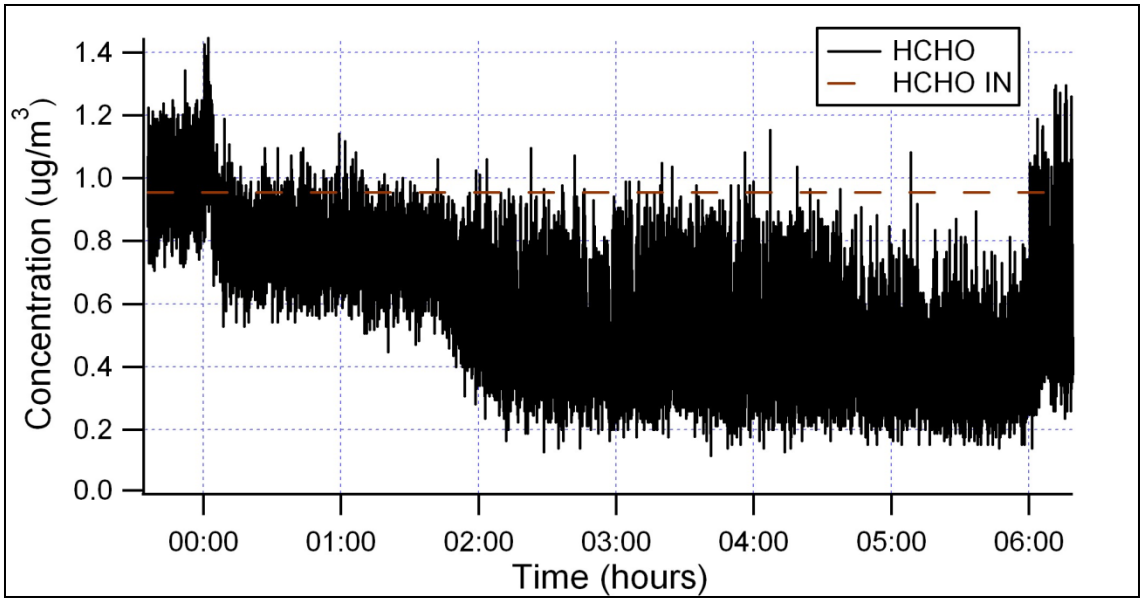

Figure 15: Concentration of Formaldehyde Over 6 Hours

Figure 16 shows the PV for the same six hour experiment. The overall PV for the experiment was 0.018 cm s^{-1}. After two hours the average PV was 0.021 cm s^{-1}. This appears to be significantly higher than the PV from the initial experiments in Figure 14. However, if the first 10 minutes of Figure 16 are compared to the 10 minutes in Figure 14 the PV and concentrations are in fact similar.

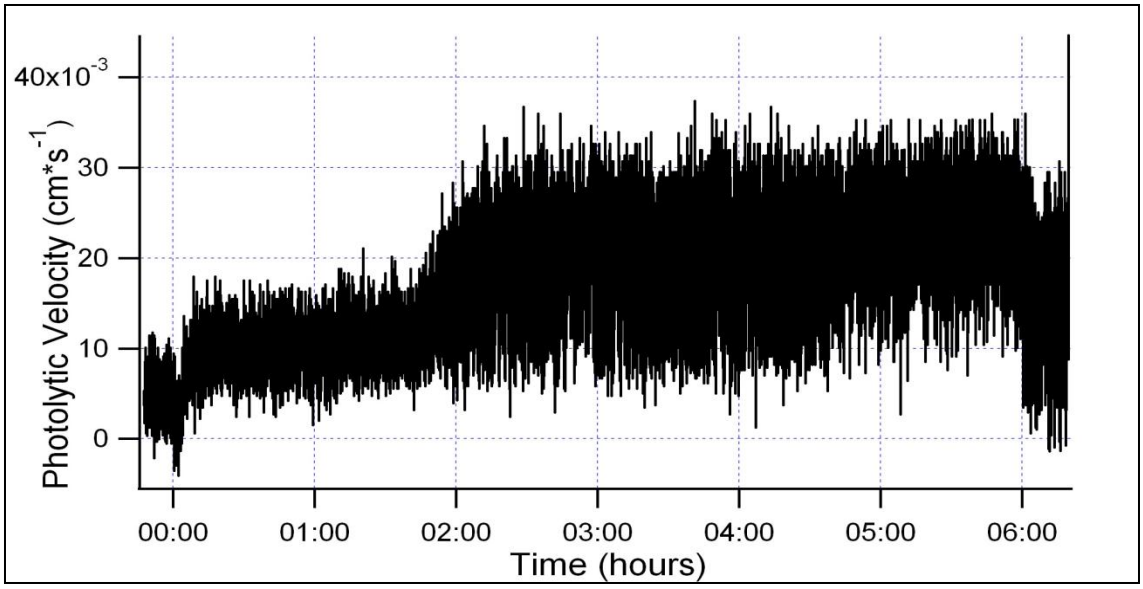

Figure 16: Photocatalytic Velocity of Formaldehyde Recorded Over Six Hours

In addition to formaldehyde, the second experiment also recorded the concentration of methanol. Standard formaldehyde solutions contain methanol to stabilize and help prevent the decomposition of formaldehyde. The proton affinity for methanol is greater than formaldehyde, and therefore the PTR-MS is more sensitive to methanol. Since the exact amount of methanol present in the formaldehyde solution was unknown the initial concentration is an approximation. Figure 17 shows the concentration of methanol over the six hour time frame. Estimating the inlet concentration from the formaldehyde sensitivity the initial concentration of methanol was 41 µg m^{-3}. After two hours the methanol concentration was reduced to approximately 13 µg m^{-3}, corresponding to a 68% decrease. Figure 18 shows the PV for methanol, which was relatively constant at 0.026 cm s^{-1} after 2 hours.

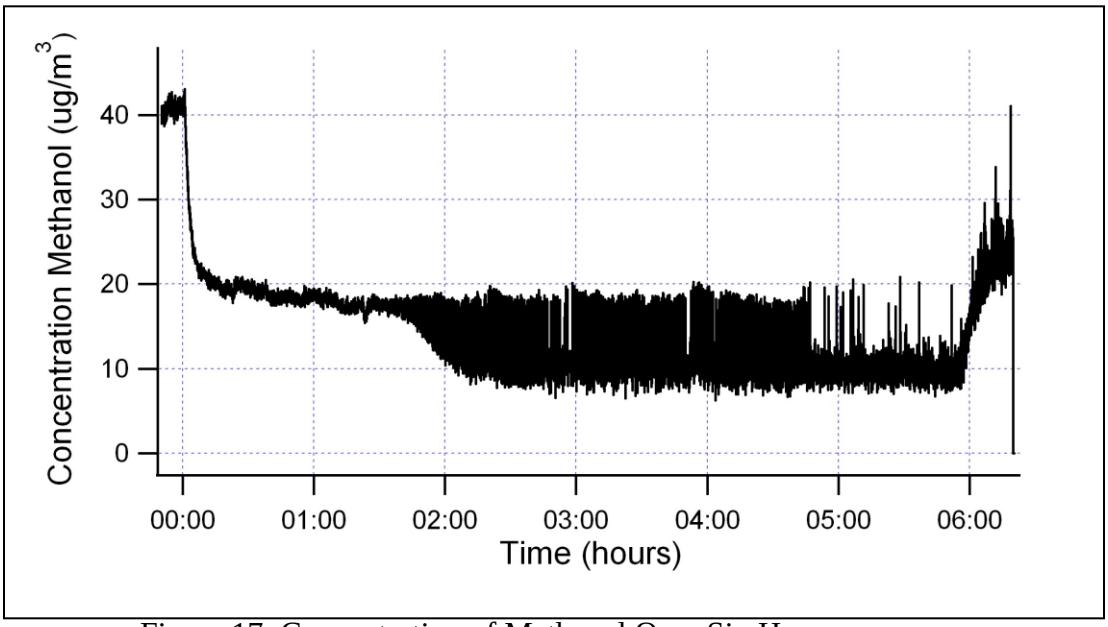

Figure 17: Concentration of Methanol Over Six Hours

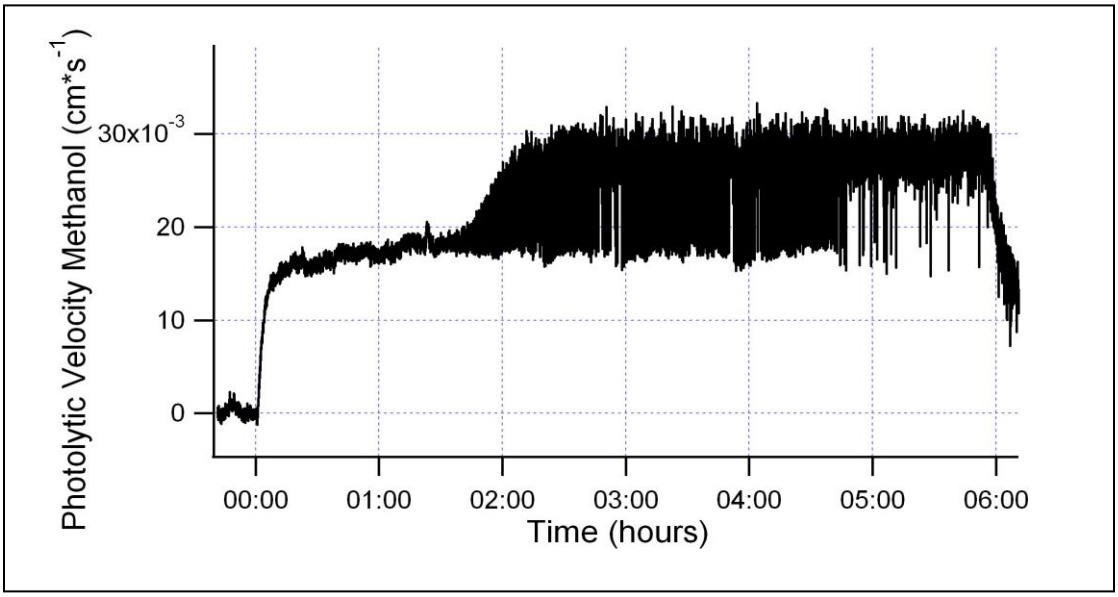

Figure 18: Photocatalytic Velocity of Methanol Recorded Over Six Hours

The third set of experiments recorded the decrease in formaldehyde levels when only 0.1 mw cm^{-2} of light illuminated the reaction cell. The decreased UV intensity mimics the amount of

light present in an indoor environment. The photolytic velocity from this experiment is shown in Figure 19. The average PV was 0.0039 cm s^{-1}. This is 15 % of the PV previously calculated. Although, a full correlation was not preformed the reduction appears to follow a linear relationship. In other words, a ten-fold reduction in UV roughly corresponds to a similar reduction in the PV.

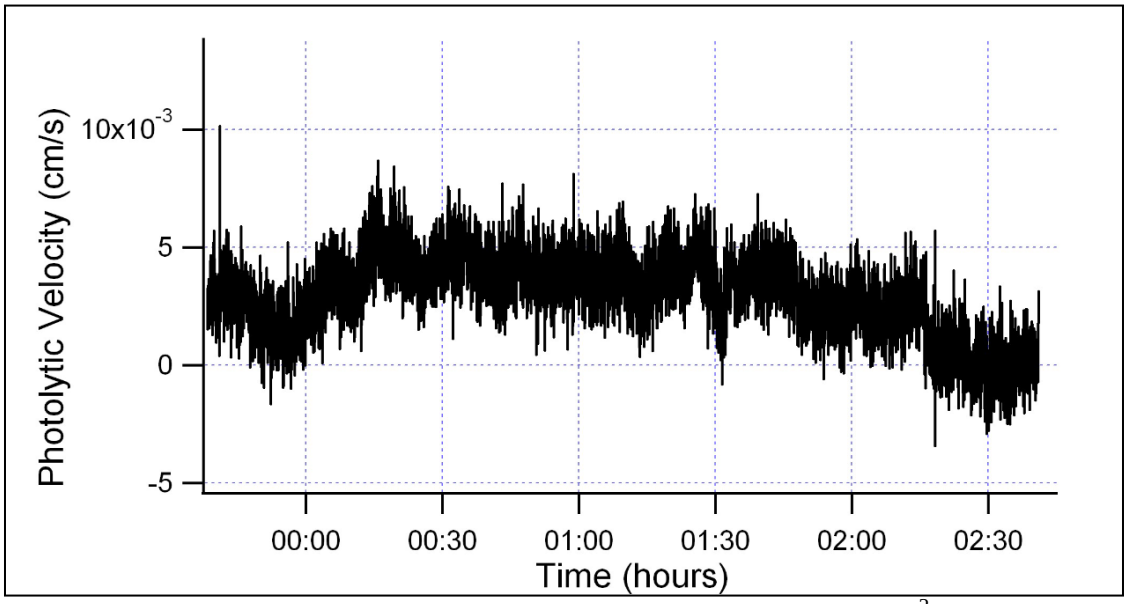

Figure 19: Photocatalytic Velocity of Formaldehyde with 0.1 mW cm^{-2} UV Intensity

The results indicate that the tiles effectively decrease the amount of formaldehyde and methanol in the flow tube. Overall, these experiments show that the tiles reduce formaldehyde by ~50% under specific laboratory conditions. A recent study optimized the reduction of formaldehyde by TiO_2 to approximately 75 % (Qi et al., 2007). However, the composition of the tiles in this experiment differed from those in the literature. In addition, the tiles reduce the methanol concentration by ~ 70%. The PV for formaldehyde and methanol are 0.018 cm s^{-1} and

0.026 cm s^{-1} respectively. Therefore the TOTO tiles could potentially be used for consistent long term formaldehyde reduction.

3.3 Chloramine Experiments

The concentration and the photolytic velocity for NH_2Cl are depicted in the graphs below. The photocatalytic velocity is dependent on NH_2Cl's mass flux to the tiles. The equation for the NH_2Cl's mass flux is based on a mass balance as described in Equation 1. Where F_{voc} is the NH_2Cl mass flux ($\mu g\ m^{-2}s^{-1}$), H is the distance from the top of the flow cell to the surface of the tiles sitting within the flow cell (0.0488 m), τ the residence time of over the tiles (96.6 s for the experiments with TOTO tiles only, and 53.43 s for concrete and TOTO tiles), C_i represents the initial concentration of NH_2Cl before it passes over the tiles, and C the concentration of NH_2Cl ($\mu g\ m^{-3}$) at the outlet of the flow cell. The photocatalytic velocity was determined using the initial concentration of NH_2Cl, and applying that to Equation 2.

3.3.1 Initial TOTO Tile Experiments

The first set of experiments irradiated the TOTO tiles for approximately two thirty-minute periods. Between each trial there was only a thirty minute recovery period. This resulted in the oscillations depicted in the graph. The PV was than calculated, and the result is shown in Figure 21. By the end of the first trial a significant photolytic velocity was reported, .040 cm s^{-1}. At the end of the second thirty minutes the PV was 0.037 cm s^{-1}. In comparison the PV for formaldehyde was 0.021 cm s^{-1}, and the PV for methanol was 0.026 cm s^{-1}.

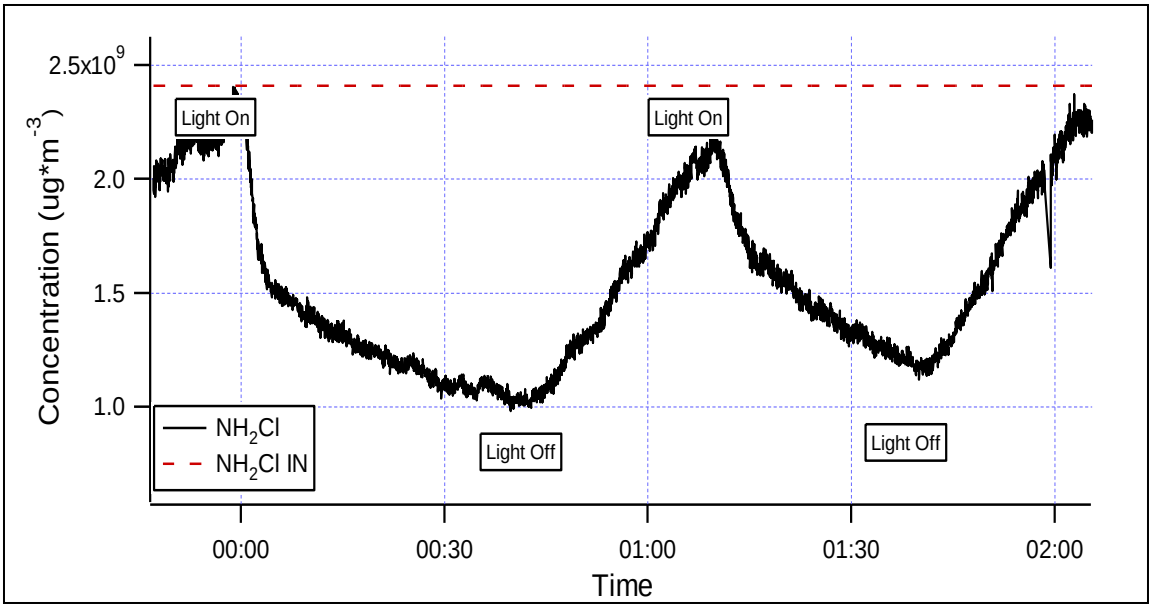

Figure 20: NH_2Cl Concentration Over Two Approximately 30 Minute Trials

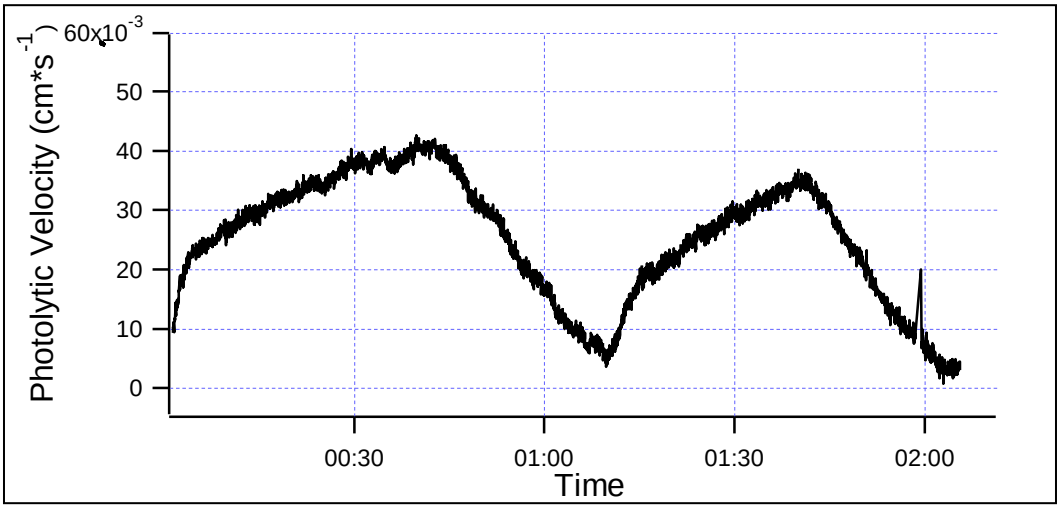

Figure 21: NH_2Cl Photolytic Velocity for 30 Minute Trials

In order to determine the effect from long term exposure the tiles were illuminated for six hours. The concentration during this time is shown in Figure 22, and the PV is seen in Figure 23. Initially the PV increases sharply after one hour. The PV reached its maximum after 2 hours, 0.045 cm s^{-1}.

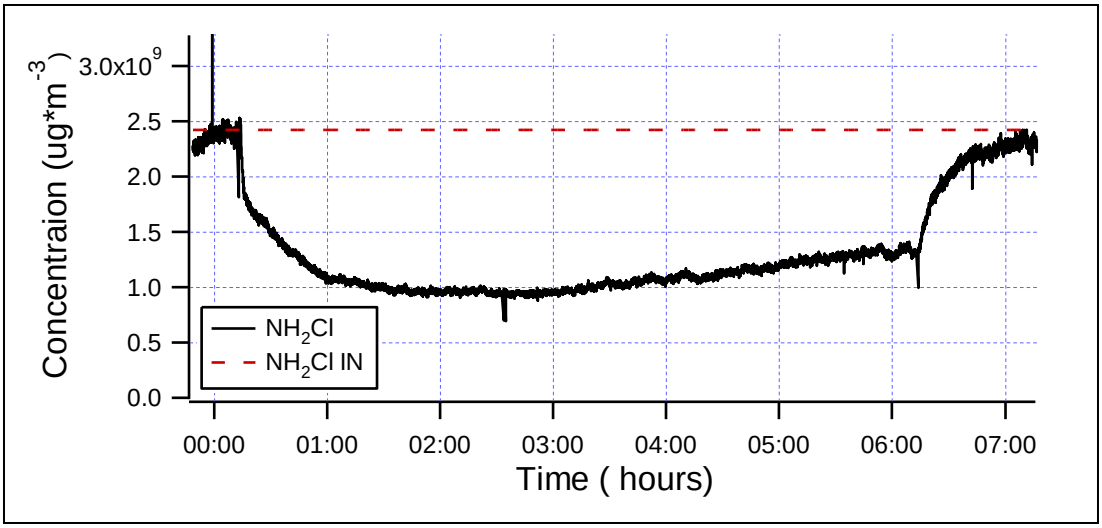

Figure 22: NH_2Cl Concentration Six Hour Trial

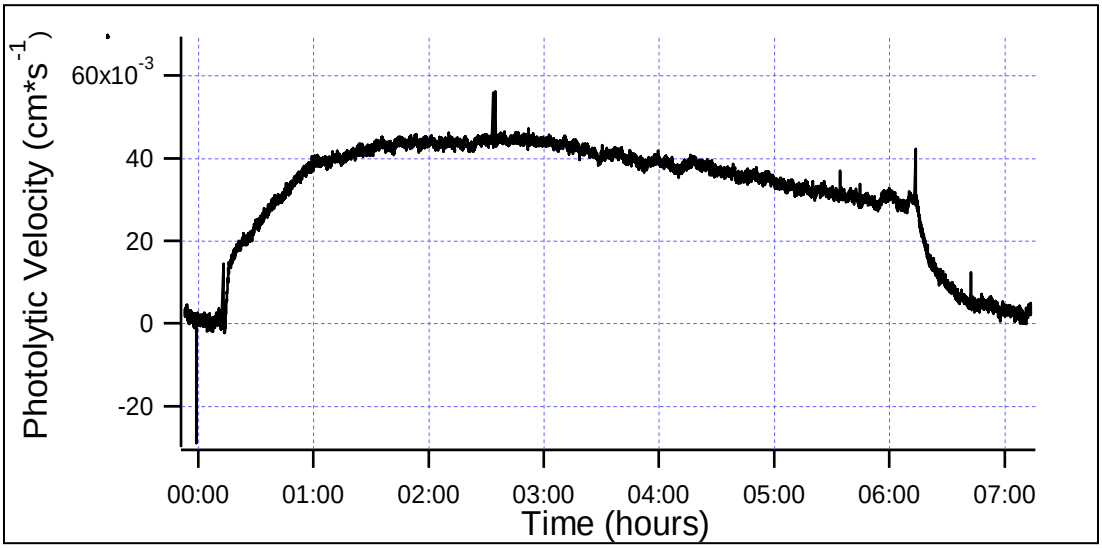

Figure 23: NH_2Cl Photolytic Velocity for Six Hour Trial

The tiles reduced the amount of NH_2Cl in the gas phase. Overall the PV remained relatively constant during the six hour time frame.

3.3.2 Concrete Tiles

Each of the concrete and TOTO samples were irradiated for both 30 minutes and three hours. The concentrations for the 30 minute and 3 hour trials were recorded, and then converted to the corresponding PV. The data from the graphs was averaged every 60 seconds to give the representation depicted below.

The PV from all of the three hour experiments is compared in Table 1. Overall the 25-5 sample has the highest PV, next to the 25-15 sample. Both the 50-5 and 50-15 sample also have a relatively high PV. All four of these samples have a higher photolytic velocity than the TOTO tile. The 25 and 50 cement samples are more efficient than the TOTO samples. The PV from the 10-5, 105-5, and 500-5 samples was less than that of the TOTO tile.

Table 1: Comparison of Averaged Photocatalytic Velocity for the Three Hour Trials

Sample	**PV * 10^{-2} ($cm*s^{-1}$) 3 Hr Experiment**
TOTO	1.77
10-5	1.68
25-5	5.37
25-15	3.72
50-5	2.39
50-15	2.06
105-5	0.897
500-5	0.989

The TOTO tiles were re-exposed to a lowered inlet concentration of 8.55 x 10^{-4} ug m^{-3}. In addition, the residence time was almost halved compared to the previous NH_2Cl experiment. Figure 24 shows the concentration for two 30 minute trials, and Figure 25 represents the corresponding PV. The increased variability characteristic of both graphs, compared to that of the previous NH_2Cl experiments, is a result of the lower inlet concentration.

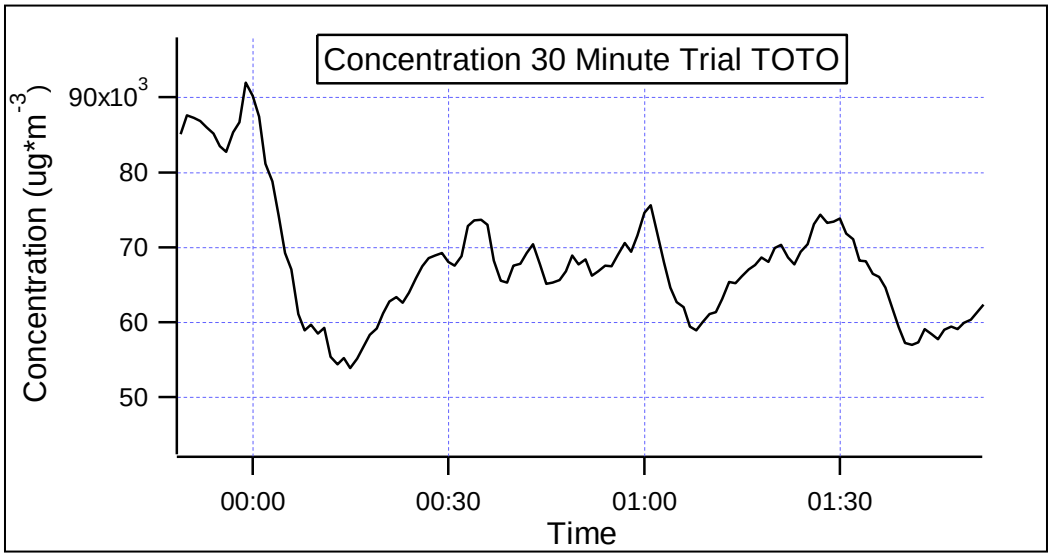

Figure 24: Concentration of Reduced NH_2Cl Over TOTO Tiles for Two 30 Minute Intervals

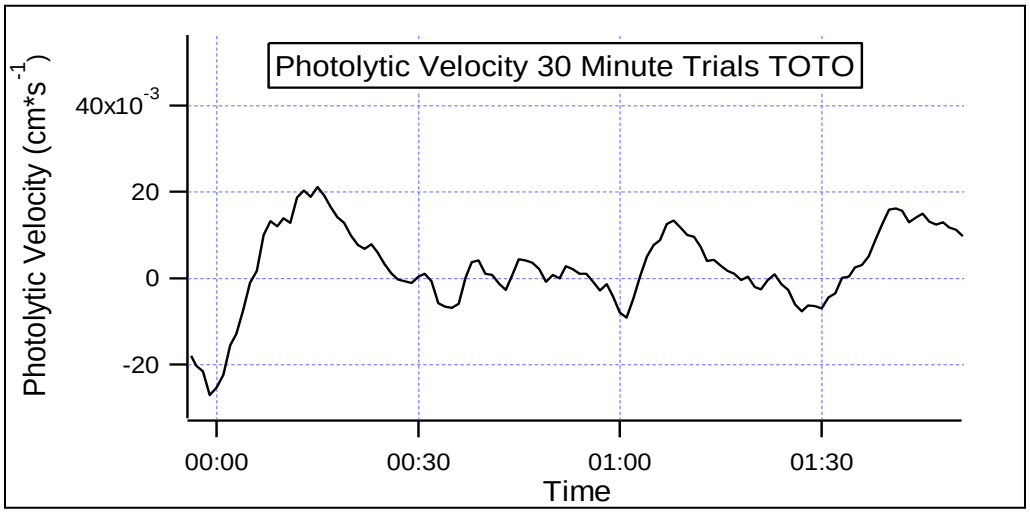

Figure 25: Photolytic Velocity Over TOTO Tiles for Two 30 Minute Intervals for Reduced NH_2Cl

Figures 26 and 27 represent the concentration and PV for the three hour exposure of the TOTO tiles, respectively. The PV averaged to 0.018 cm s^{-1}. This is slightly less than half of the PV from the previous experiment. The PV is lower due to the lowered residence time found in Equation 1. By lowering the residence time the tiles were exposed to less NH_2Cl, and this corresponds to a lowered overall PV. The results from this trial were compared with the results from the later concrete sample experiments.

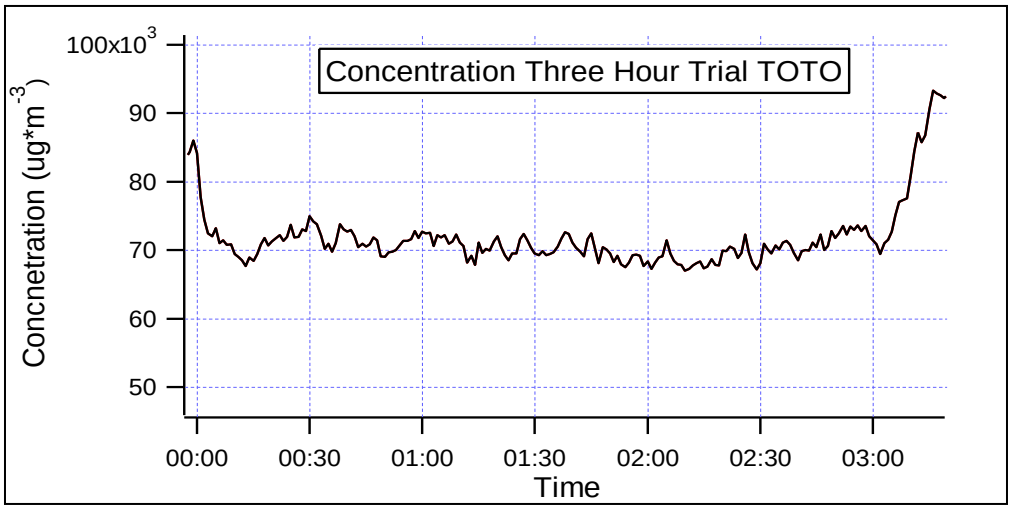

Figure 26: Concentration of NH_2Cl for 3 Hours Over TOTO Tiles

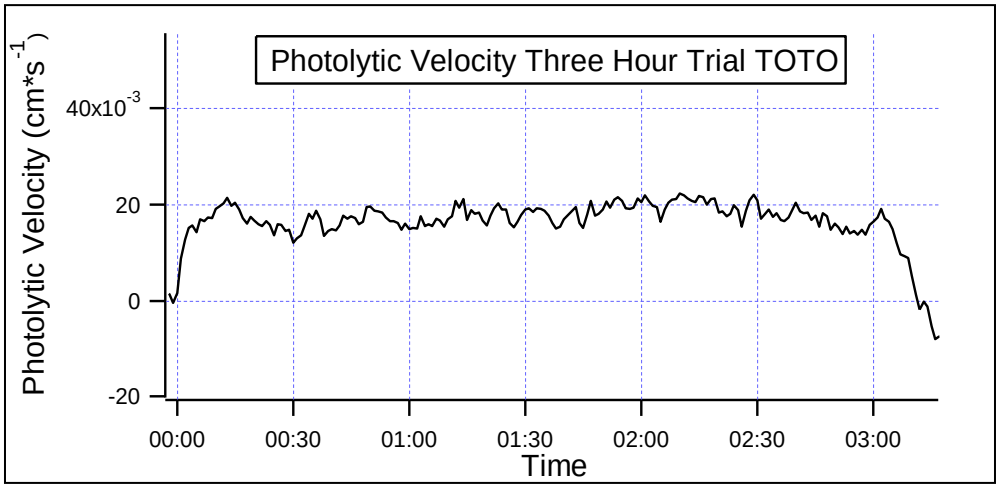

Figure 27: Photolytic Velocity of NH_2Cl for 3 Hours Over TOTO Tiles

Figures 28-31 show the results from the two experiments on the 10-5 concrete samples. Figures 28 and 29 respectively represent the change in concentration and PV for the 10-5 concrete samples after 30 minutes of exposure. Figure 28 depicts two trials, as will all subsequent 30 minute trial graphs. The captions on the graph indicate when the light was turned on and when it was again turned off. These trials show that the results could be replicated. The 10-5 samples were irradiated for three hours. The results are shown for the concentration, Figure 30, and the PV, Figure 31. These figures show a steady decrease for the three hour period. This might suggest that the trial should be run for longer. In an earlier experiment, not shown below the tiles were irradiated for 6 hours, and after the first three the outlet concentration leveled off. Therefore, although the average PV for the time frame is 0.013 cm s^{-1}, the PV for the last 60 minutes was 0.017 cm s^{-1}. This number corresponds to the PV from the 6 hour trial.

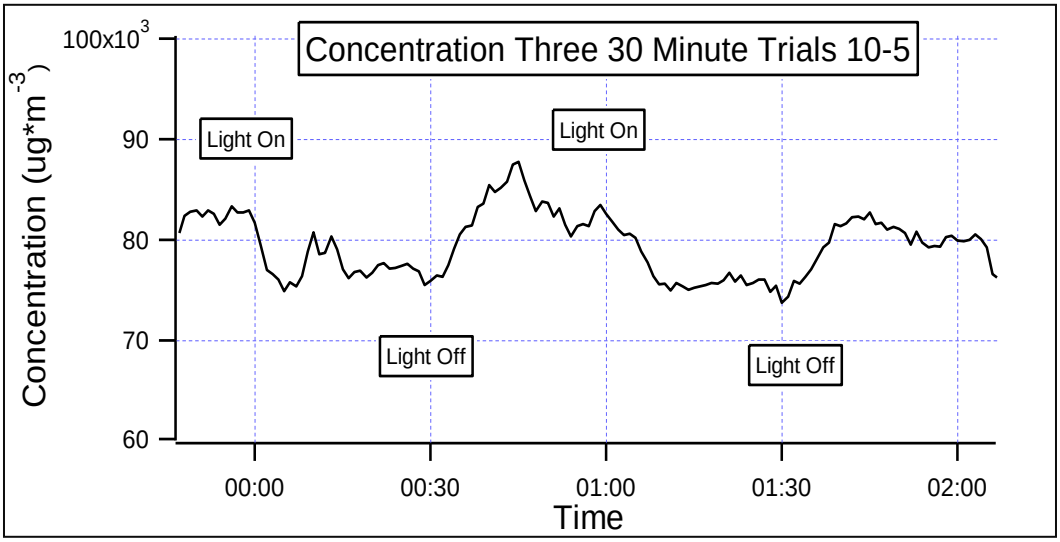

Figure 28: Concentration of NH_2Cl for 30 Minutes Over 10-5 Concrete

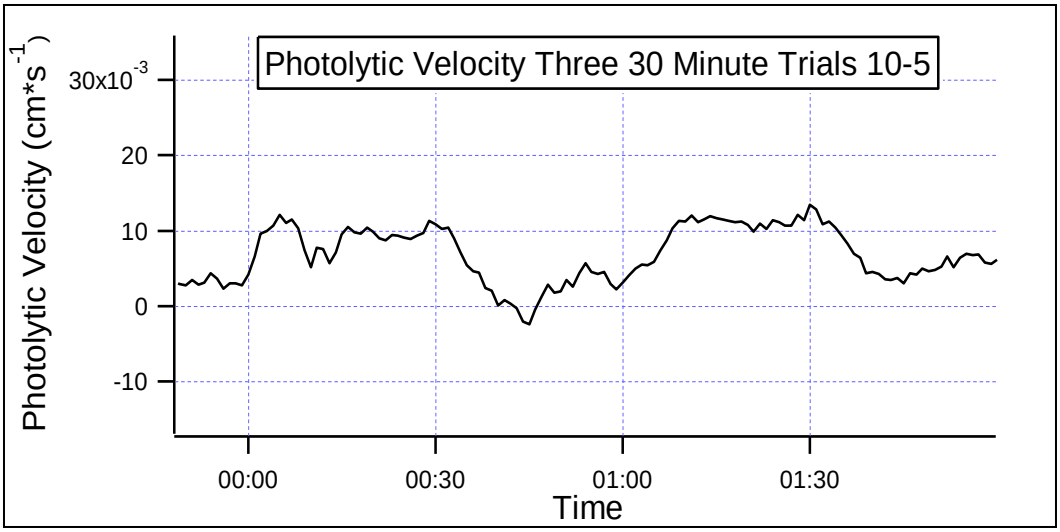

Figure 29: Photolytic Velocity of NH_2Cl for 30 Minutes Over 10-5 Concrete

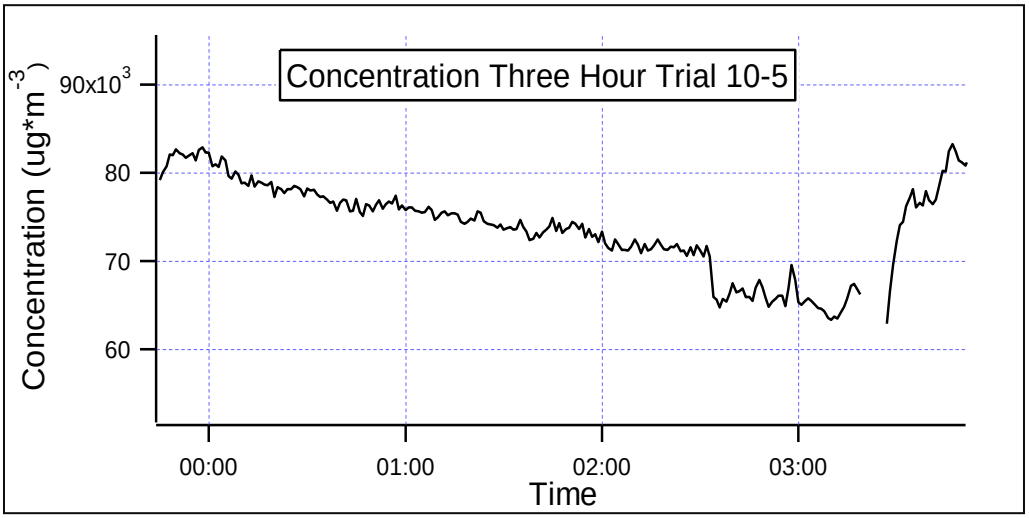

Figure 30: Concentration of NH_2Cl for 3 Hours Over 10-5 Concrete

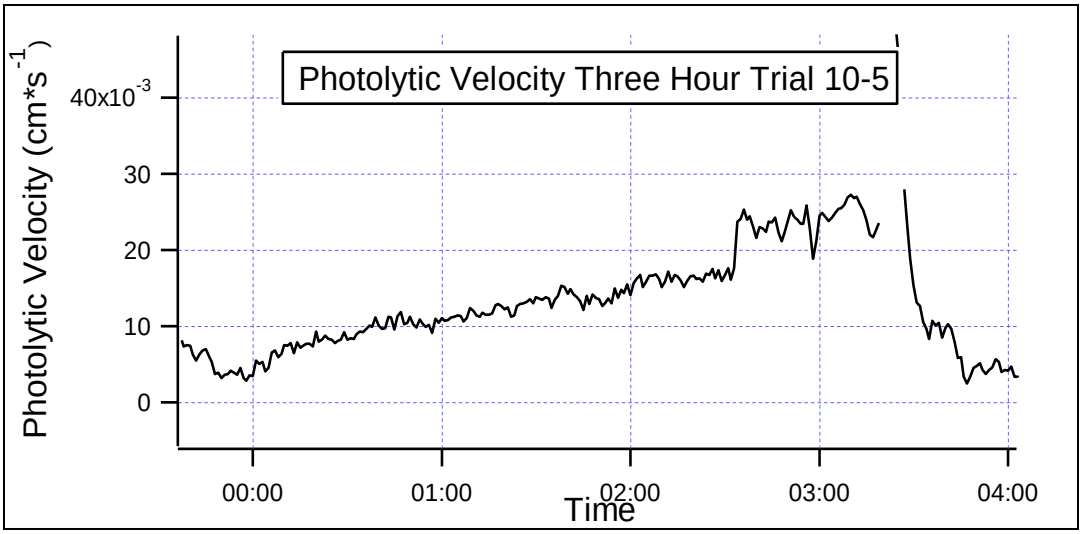

Figure 31: Photolytic Velocity of NH_2Cl for 3 Hours Over 10-5 Concrete

The 25-5 samples gave the largest decrease in NH_2Cl, Figures 32-35. The concentration and PV from the 30 minute trials are represented in Figures 32 and 33 respectively. The decrease is dramatic and rapid. In addition, the amount reduced remained generally constant, and has only a small amount of variability. In the three hour trial the outlet concentration stayed constant for the duration of the experiment, as seen in Figure 34. The overall PV from this experiment was 0.054 cm s^{-1}, Figure 35 represents this. This PV is larger than the TOTO tiles, or any other concrete sample. Therefore, 25-5 concrete, (P25 concrete - 5 % TiO_2 by weight), is the best at reducing NH_2Cl in the gas phase.

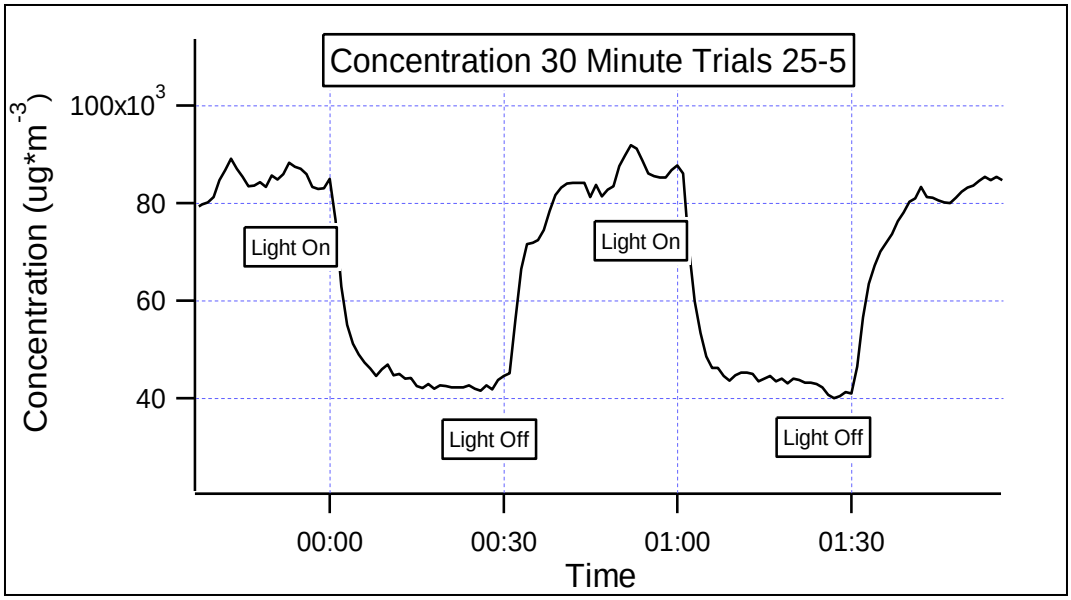

Figure 32: Concentration of NH_2Cl for 30 Minutes Over 25-5 Concrete

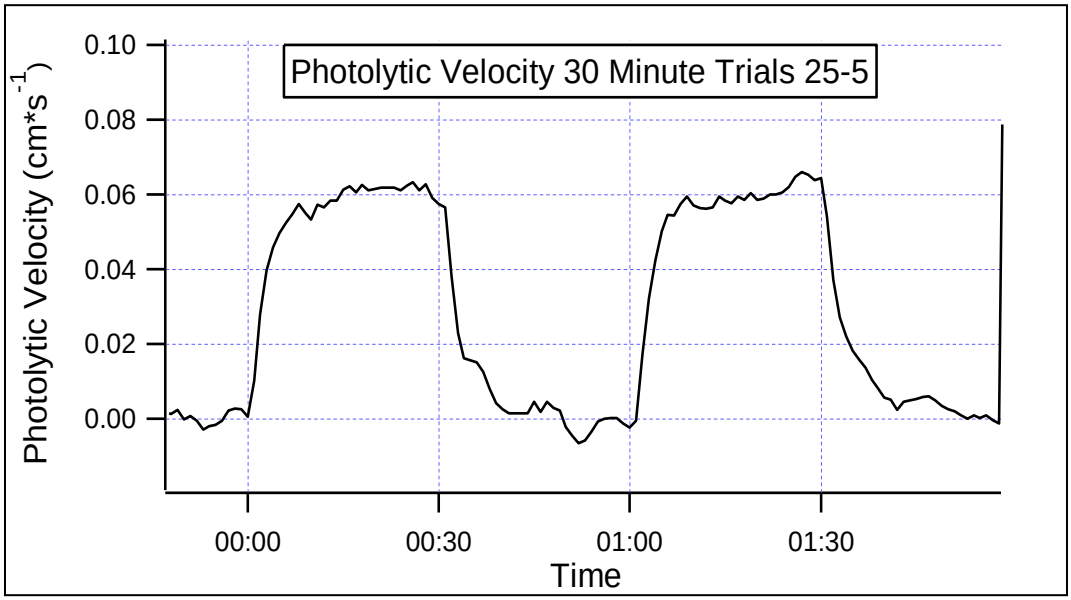

Figure 33: Photolytic Velocity of NH_2Cl for 30 Minutes Over 25-5 Concrete

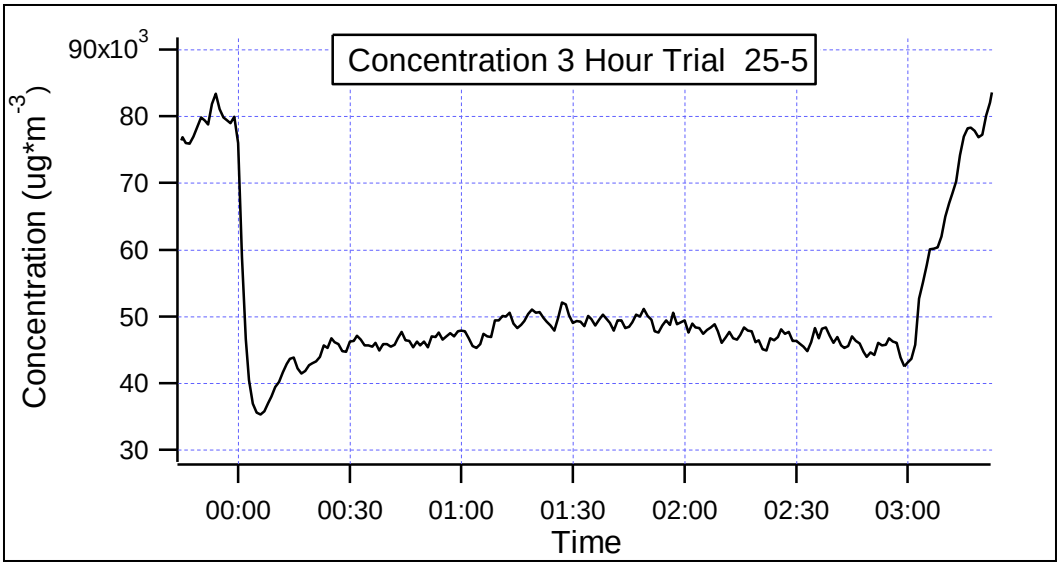

Figure 34: Concentration of NH_2Cl for 3 hours Over 25-5 Concrete

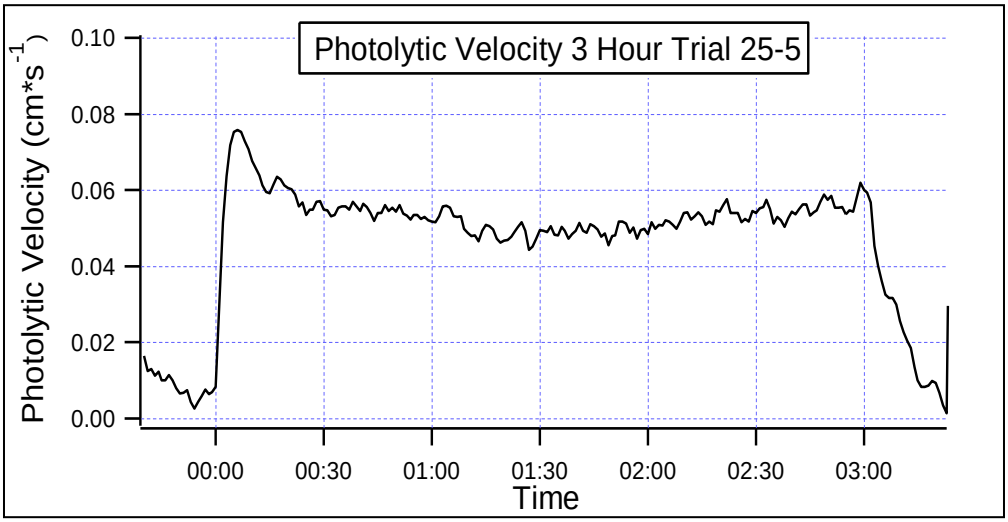

Figure 35: Photolytic Velocity of NH_2Cl for 3 hours Over 25-5 Concrete

The 25-15 concrete sample also effectively reduced NH_2Cl in the gas phase, as seen in Figures 36-39. Figures 36 and 37 show the results from the 30 minute trial with the 25-15 concrete samples. Figure 36 displays the concentration for this time period, and Figure 37 shows the PV. Figures 38 and 39 represent the concentration reduction and the PV from the 3 hour trial, respectively. In Figure 39 the 3 hour PV averaged to 0.038 cm s^{-1}. This is lower than the PV

from the 25-15 experiments. This is counterintuitive; since the 25-15 samples have 15 % TiO_2 compared to the 5% TiO_2 in the 25-5 samples it would follow that the 25-15 sample would have a higher PV. However, in both the thirty minute trial and the three hour trial the PV for the 25-15 sample is lower. The reason for this is unknown. Nonetheless, the 25 concrete type is the most effective at reducing monochloramine, as will become evident.

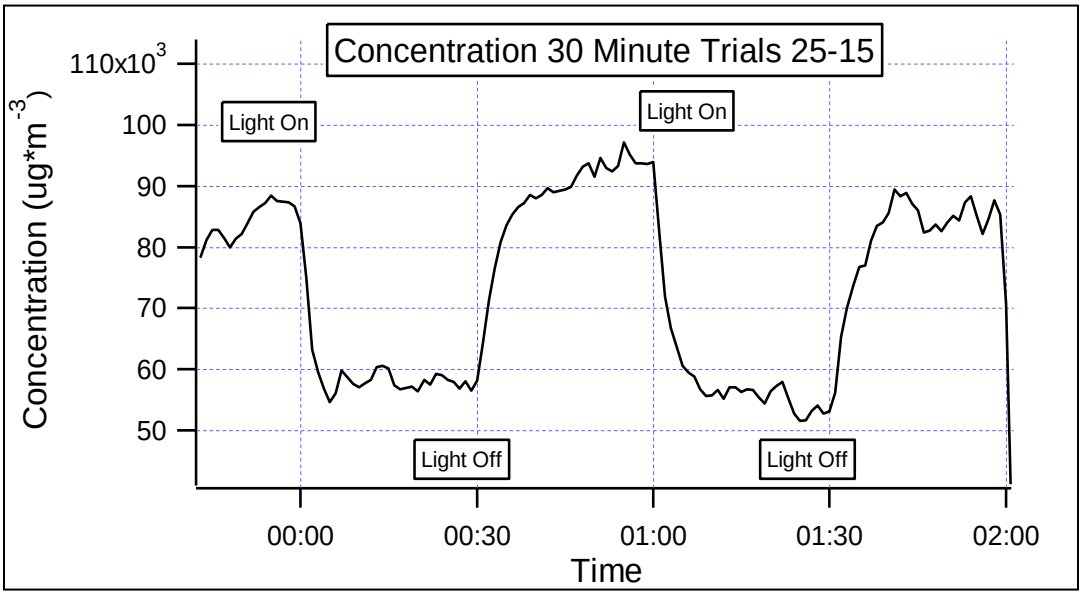

Figure 36: Concentration of NH_2Cl for 30 Minutes Over 25-15 Concrete

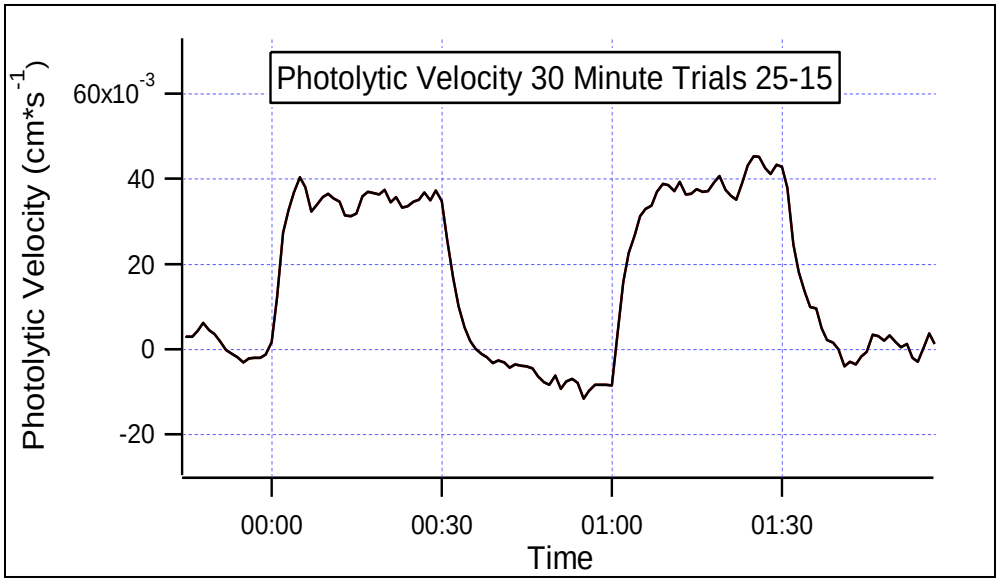

Figure 37: Photolytic Velocity of NH_2Cl for 30 Minutes Over 25-15 Concrete

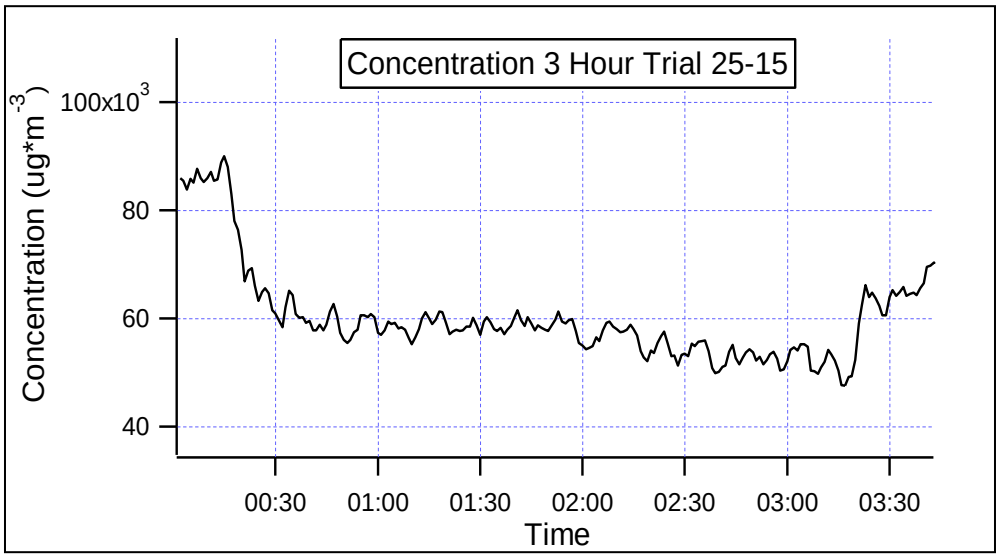

Figure 38: Concentration of NH_2Cl for 3 Hours Over 25-15 Concrete

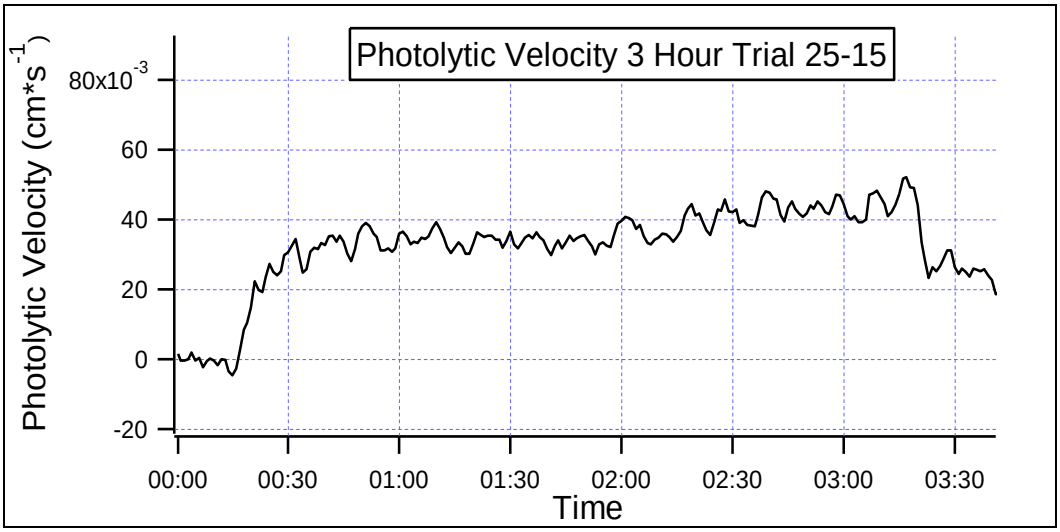

Figure 39: Photolytic Velocity of NH_2Cl for 3 Hours Over 25-15 Concrete

The results from the experiments with the 50-5 sample are shown in Figures 40-43. Figure 40 and Figure 41 depict the concentration and PV from the 30 minute trial. The PV for the 50-5 sample is lower than the PV from the 25-5 and 25-15 samples. The concentration from the 3 hour trial is shown in Figure 42, and the PV in Figure 43. The average PV for the 50-5 sample was 0.024 cm s^{-1}. This is higher than the TOTO and 10-5 samples. Therefore the 50-5 samples still significantly decrease the amount of gaseous NH_2Cl.

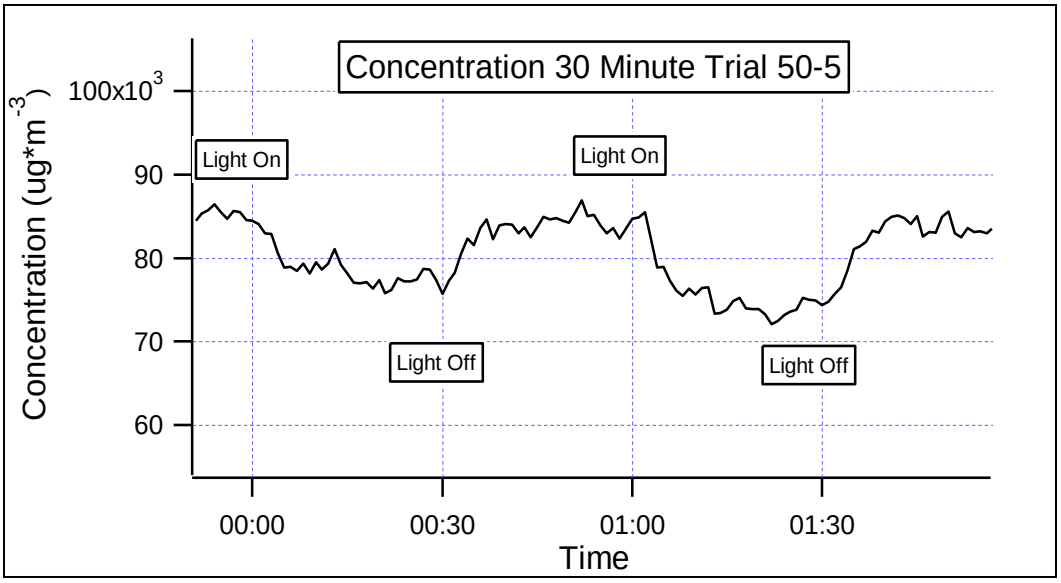

Figure 40: Concentration of NH_2Cl for 30 Minutes Over 50-5 Concrete

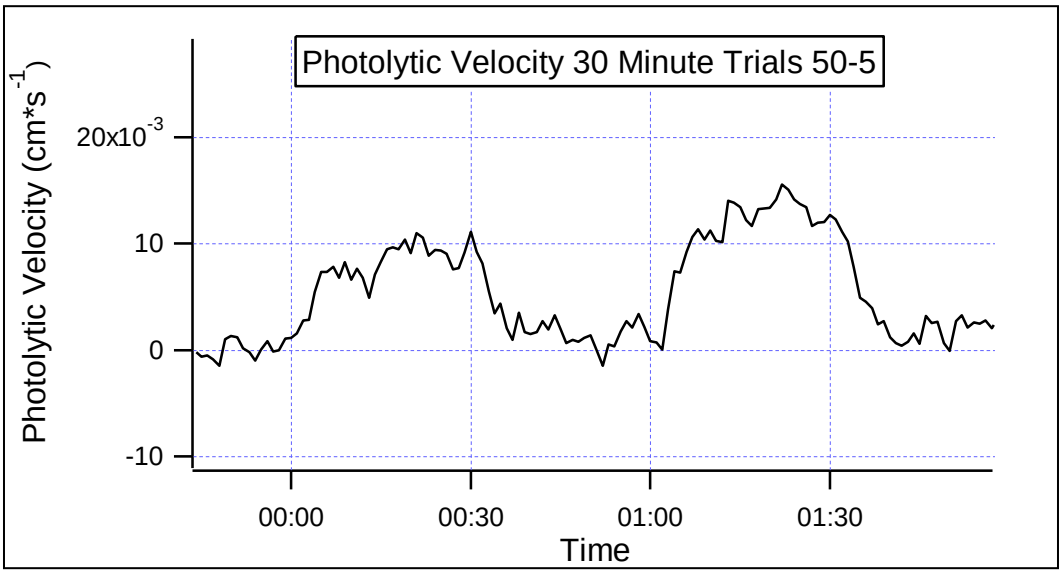

Figure 41: Photolytic Velocity of NH_2Cl for 30 Minutes Over 50-5 Concrete

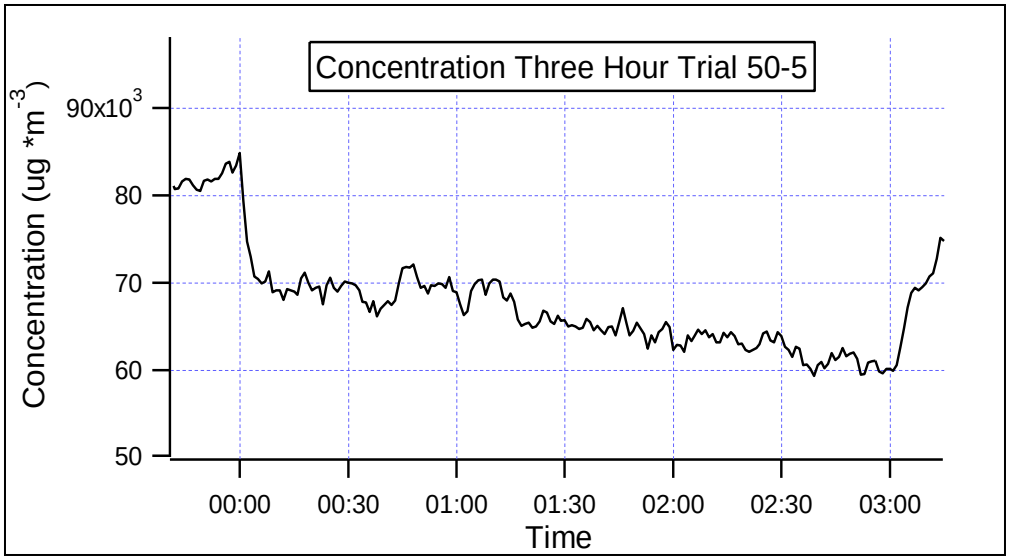

Figure 42: Concentration of NH_2Cl for 3 Hours Over 50-5 Concrete

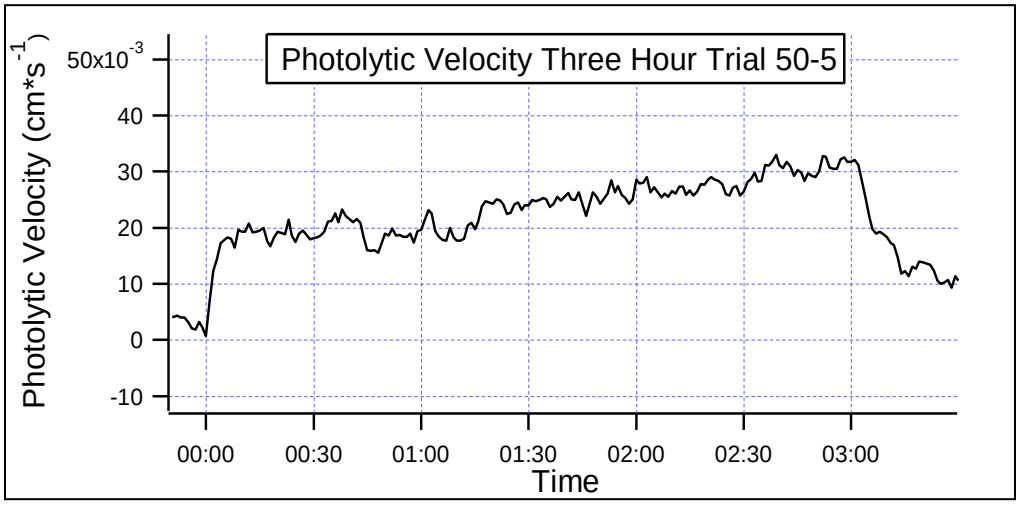

Figure 43: Photolytic Velocity of NH_2Cl for 30 Minutes Over 50-5 Concrete

The experiments with the 50-15 samples are depicted in Figures 44-47. For the three hour experiment with the 50-15 samples the PV was 0.021 cm s^{-1}, Figure 47. This is slightly lower than that found with the 50-5 sample; however, the PV is close enough that they are almost interchangeable. Nonetheless, both 50-5 and 50-15 underperform compared to the 25-5 and 25-15 samples.

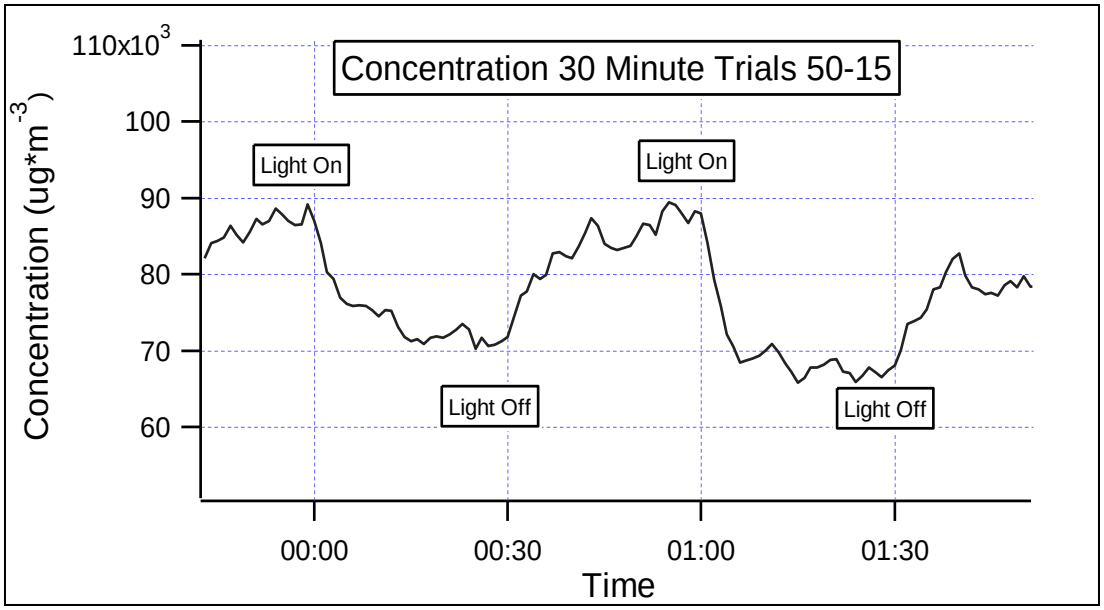

Figure 44: Concentration of NH_2Cl for 30 Minutes Over 50-15 Concrete

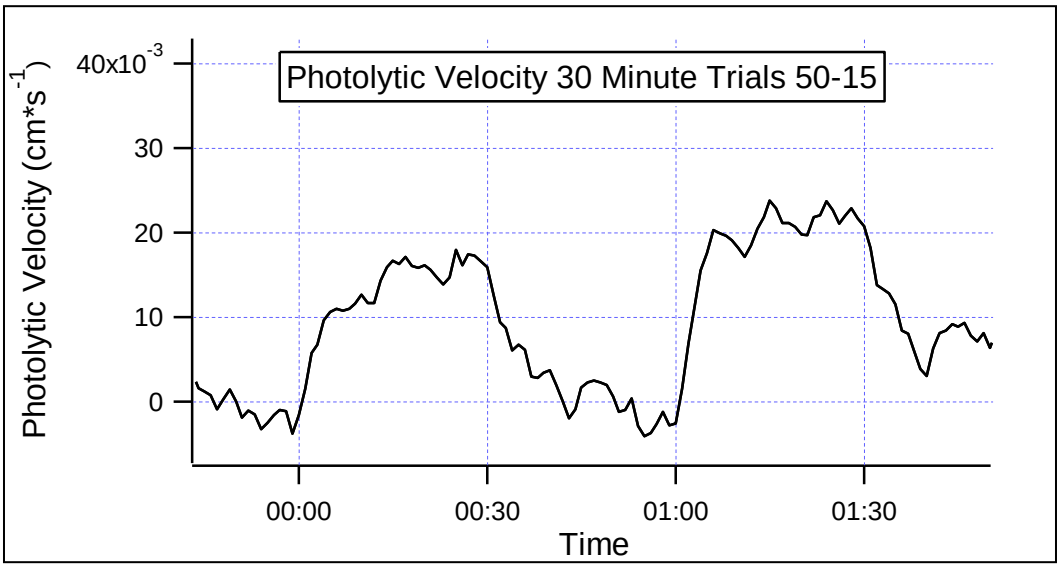

Figure 45: Photolytic Velocity of NH_2Cl for 30 Minutes Over 50-15 Concrete

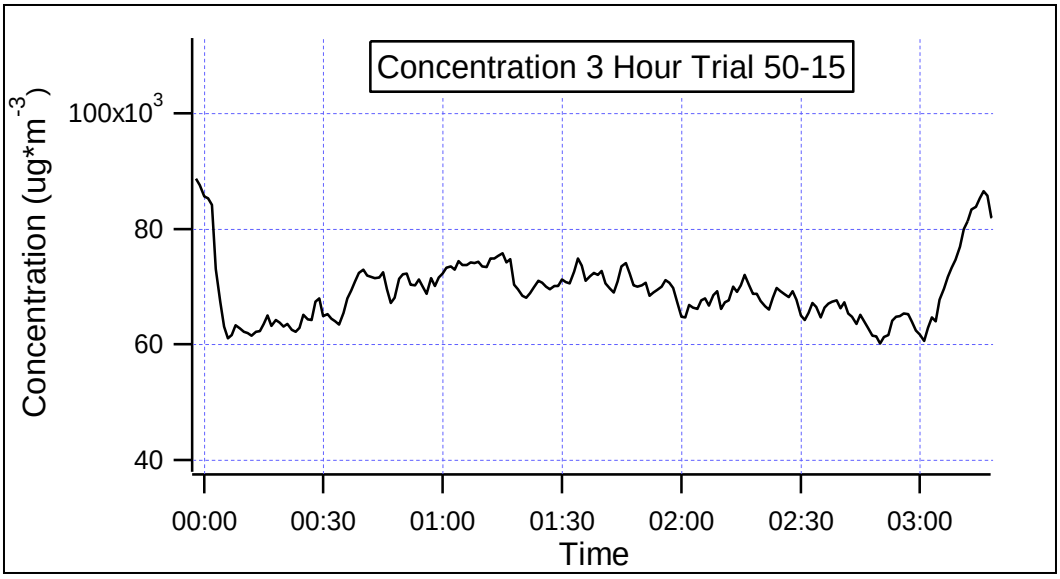

Figure 46: Concentration of NH_2Cl for 3 Hours Over 50-15 Concrete

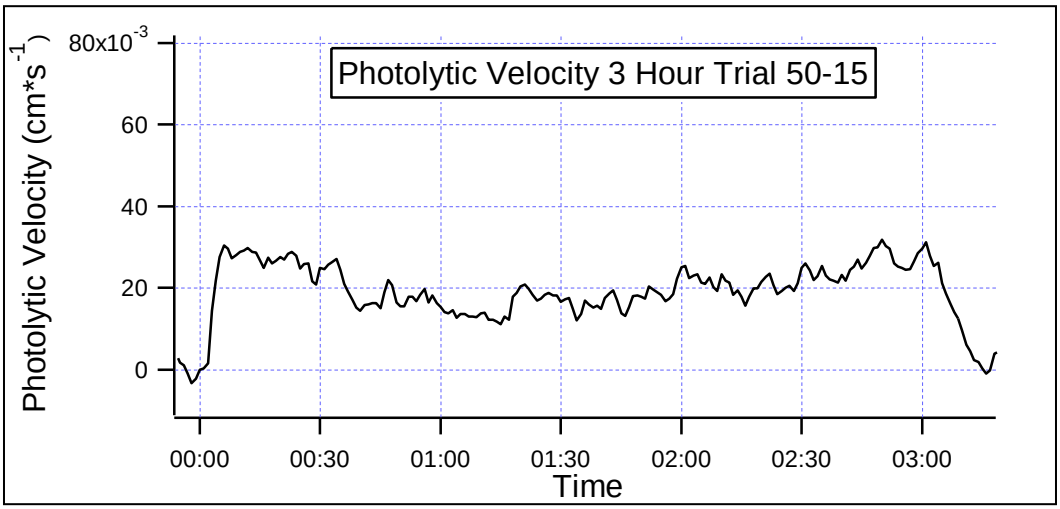

Figure 47: Photolytic Velocityof NH_2Cl for 3 Hours Over 50-15 Concrete

The 105-5 concrete was the least effective at reducing NH_2Cl, as shown in Figures 48-51. The concentration reduction from the 30 minute experiment is shown in Figure 48, and the PV from that experiment is shown in Figure 49. It appears that after the initial reduction the concentration fluctuates. After the 30 minute trials the concentration oscillated, as seen in Figure 50. The PV from the 30 minute trial, Figure 49, appears higher than the PV from the 3 hour trial

seen in Figure 51. After the initial reduction the PV does not steady. Overall the average PV for the 3 hour trial was 0.90 cm s^{-1}.

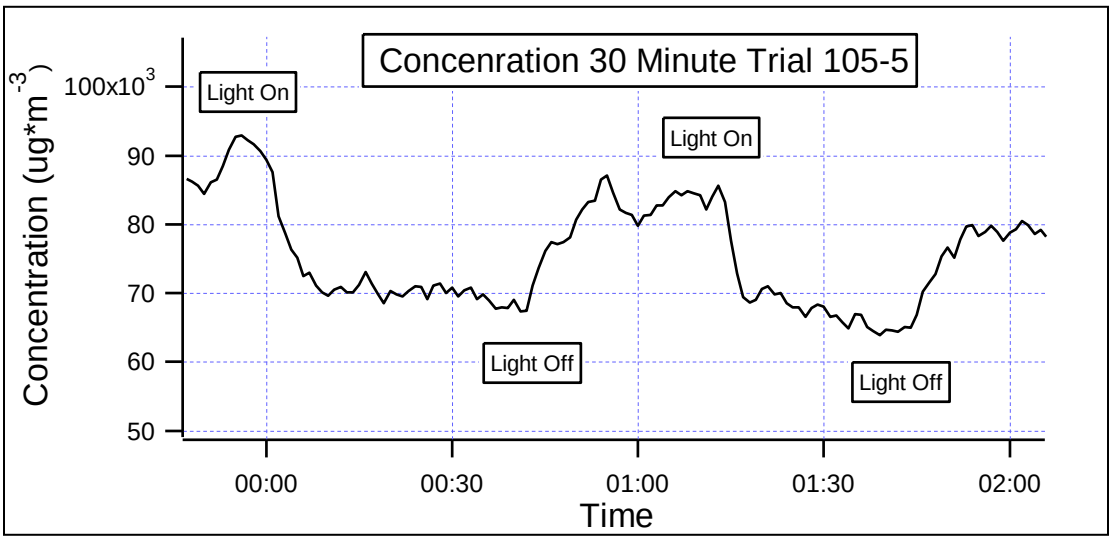

Figure 48: Concentration of NH_2Cl for 30 Minutes Over 105-5 Concrete

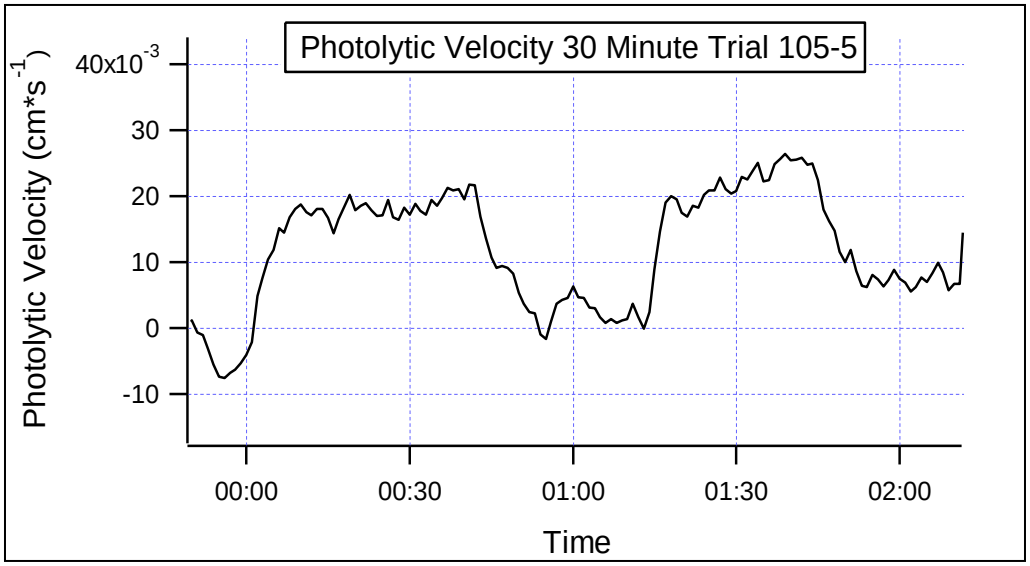

Figure 49: Photolytic Velocity of NH_2Cl for 30 Minutes Over 105-5 Concrete

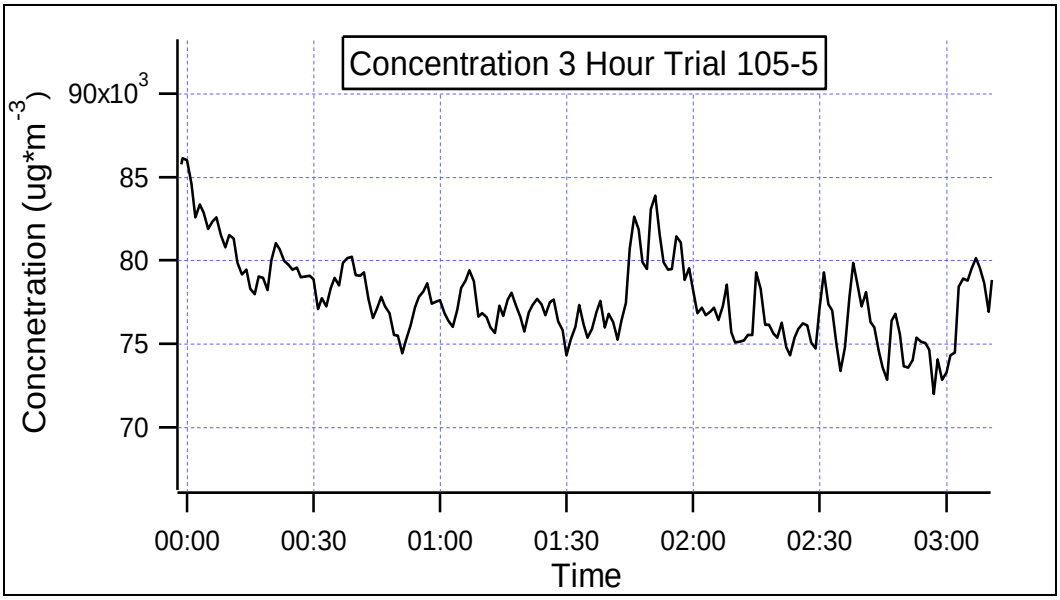

Figure 50: Concentration of NH_2Cl for 3 Hours Over 105-5 Concrete

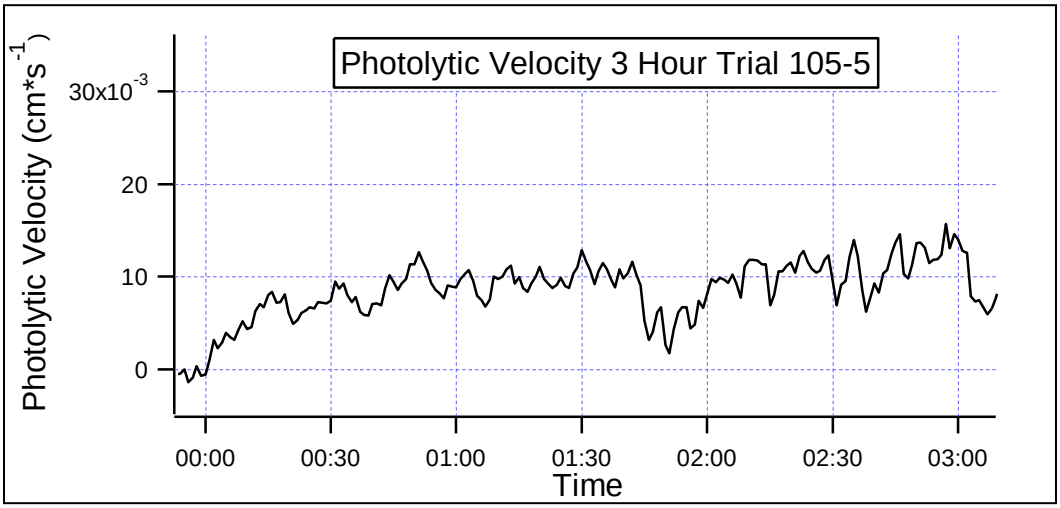

Figure 51: Photolytic Velocity of NH_2Cl for 3 Hours Over 105-5 Concrete

The results from the experiments on the 500-5 concrete samples are shown in Figures 52-55. The concentration decrease, Figure 52, and the PV change, Figure 53, from the 30 minute trial correlate with the results from the 3 hour trial, Figures 54 and 55. The concentration decrease in both cases is small, Figures 52 and 54. Overall the PV in Figure 55 from the 3 hour trial is 0.99 cm s^{-1}.

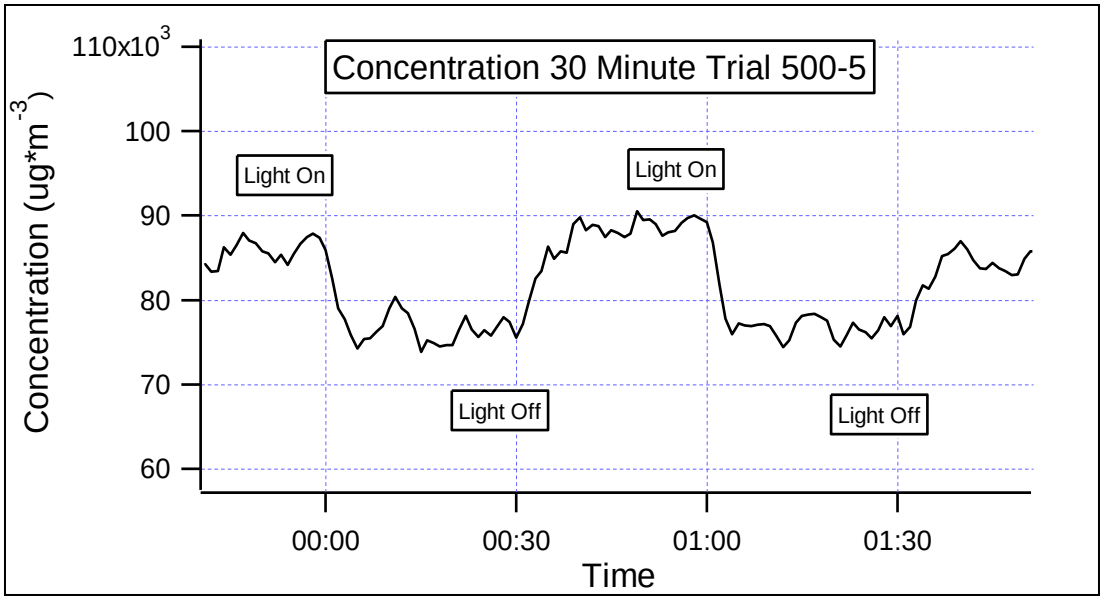

Figure 52: Concentration of NH_2Cl for 30 Minutes Over 500-5 Concrete

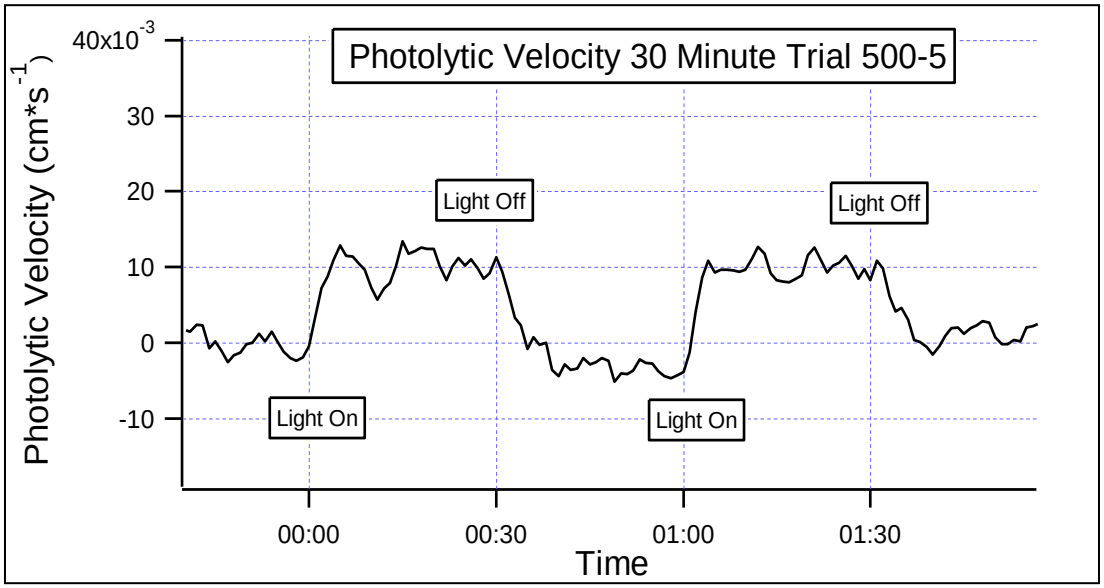

Figure 53: Photolytic Velocity of NH_2Cl for 30 Minutes Over 500-5 Concrete

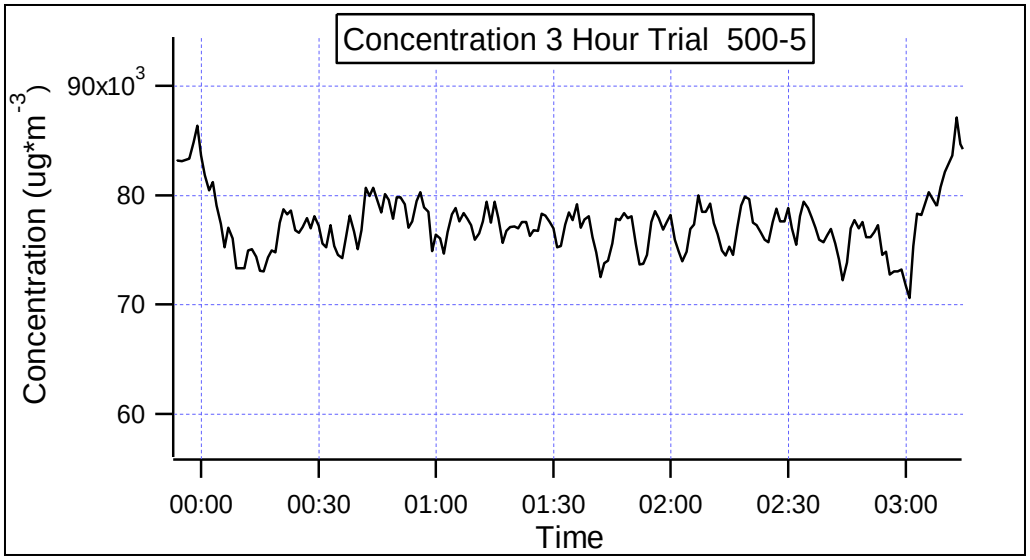

Figure 54: Concentration of NH_2Cl for 3 Hours Over 500-5 Concrete

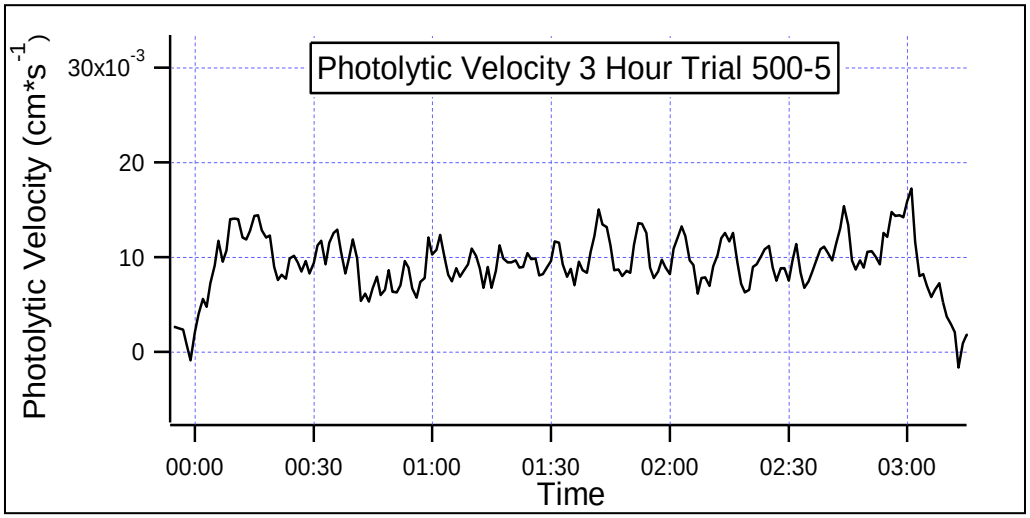

Figure 55: Photolytic Velocity of NH_2Cl for 3 Hours Over 500-5 Concrete

To determine the overall mass balance of Cl, the TiO_2 surfaces were extracted and analyzed. After the tiles were illuminated for 3 hours they were washed with 100 mL of ultrapure deionized water. These samples were then analyzed in an ion chromatograph, (IC). The results for all of the samples are listed in the second column of Table 2. Over the three hour time frame, 22.3 mg of total chlorine entered the cell. Therefore an approximate percentage of total chlorine

was converted and deposited onto tiles surface in the form of chloride (Cl^-), these percentages are listed in the second column of Table 2. This percentage indicates the fraction of the total deposition that was converted to HCl. A sizable deposition of HCl could result in long-term damage to the surfaces.

A closer analysis of the results in Table 2 reveals a positive correlation between the PV and the amount of chloride deposited. A linear regression of the PV and chloride concentration for only the concrete samples, (excluding the TOTO tiles), results in an R value of 0.64. The relationship results in a positive slope; however a linear regression may not be the best representation of the data. The 25 concrete samples had the most deposited Cl^-, and the 10-5, 105-5 and 500-5 samples had the least amount deposited. However, the TOTO tile had the largest amount of chloride on its surface, despite its lower PV. This may be a false bias that resulted from the differences in the samples surfaces. The concrete samples may retain chloride and other ions deposited on their surfaces more than the tile. This might be attributed to the fact that the tile surface was smoother than, and less porous than that of the concrete. If that is the case, then the production of HCl on the concrete surface would be more detrimental, since it would not wash easily from the surface. However, this remains a hypothesis. In addition, the composition of the two samples was different. The concrete samples have additional atoms including calcium. Also, the tile samples localized the TiO_2 to the top surface, whereas the TiO_2 in the concrete was uniformly distributed. Although, this should not affect the overall PV, since the reaction occurs on the sample surface, it does highlight the fact that the two samples are not uniform. There is a difference between the TOTO tiles and the concrete samples. Both are effective at reducing NH_2Cl, but the surface characteristics and other factors, such as porosity

and the distribution of TiO_2 on the tiles surface, may influence the reaction rates and the photolytic velocity.

Table 2: Ion Chromatograph Results from the Three Hour Trials

Sample	**Concentration Chloride (mg Deposited)**	**Percentage of Total Chlorine Mass**
TOTO	0.0517	0.233%
10-5	0.00923	0.041%
25-5	0.0231	0.103 %
25-15	0.0289	0.129 %
50-5	0.0203	0.091 %
50-15	0.0185	0.082%
105-5	0.0112	0.050%
500-5	0.00849	0.038%

3.4 Ultrafine Particle Condensation

Although the TiO_2 tiles reduced NO_X in the gas phase, it was hypothesized that the tiles could concurrently produce ultrafine particles, having a potentially negative impact on air quality. Ultrafine particles have a diameter less than 0.1 μm, and although they may not have a high mass count they can have a very high number count in urban environments. These particles are a particular health threat since they can deposit in the deep lungs. The ultrafine particles are not cleared from the lung by macrophages, and extended interaction between the particles and epithelial cells lining the lung causes inflammation (Oberdorster, 2001). Also, the large amount of surface area in contact with the lung increases the opportunity for additional surface reaction.

This results in inflammation, and eventually leads to lung disease (Oberdorster, 2001). In addition, occupational exposure can result in heart rate variability, systematic inflation, and perhaps congestive heart failure (Fang, 2010). At a lower dose residential traffic exposure was shown to increase blood pressure (Rioux, 2010).

The experiment was conducted to determine if any ultrafine particles were produced. The photocatalytic reaction that occurs on the tile surface produces hydroxyl radicals, as explained above, these radical species contribute to secondary particle formation. Primary particles are generated from biogenic and anthropogenic sources. However, secondary particles form by gas-to-particle conversion in the atmosphere. Once a molecule reacts with OH or ozone it will generate a compound that will partition itself between the gas and aerosol phases. Hydroxyl radicals can oxidize numerous gas-phase compounds that result in the formation of aerosols and fine particles. These radical species react with hydrocarbons to generate semi-volatile organics, or SO_2 to form particulate H_2SO_4. In addition, $OH\cdot$ reacts with NO_2 to produce HNO_3, and will go on to produce particulate NH_4NO_3 in the presence of ammonia (Heinsohn and Kablel, 1999). Although, hydroxyl radicals reduce the concentration of gaseous pollutants, they could significantly increase the particulate concentration.

The average results from the Condensation Particle Counter are listed in Table 3. The results were recorded in particles per cubic centimeter. Although, the counts fluctuated during different times in the day, as is expected, the production of ultrafine particles was less than expected. At certain times during the day the particle counts were less than the reference. In the morning the counts increased slightly after the tiles were illuminated. However, in the afternoon the counts were similar to those without the light on. In the evening the counts decreased. Therefore the counts recorded from this study are inconclusive. The reaction rates on the surface

of the TiO_2 were not analyzed, but could offer additional insight. The results presented here are suggestive, and additional trials and experiments are needed to understand the overall effect.

Table 3: Ultrafine Particle Counts

Light	Time	Averaged Counts (# cm^{-3})
Off	9:50	1564.8
On	9:51- 10:07	2971.44
Off	10:20	2297.18
Off	12:20	2909.08
On	12:21-12:41	3315.95
Off	14:34	2542.93
On	14:35-14:55	2499.5
Off	13:15	1732.5
Off	16:57	4265.07
On	17:05-17:25	2663
Off	17:40	3107.5

CHAPTER 4

CONCLUSION AND FUTURE ANALYSIS

The TiO_2 tiles effectively reduced three families of gaseous pollutants. A comparison of the photocatalytic velocity reveals the tiles were most effective at reducing monochloramine as compared to NO_x and specific VOC's (formaldehyde and methanol). The PV values for laboratory generated NO and NO_2 were 0.016 cm s^{-1} and 0.0015 cm s^{-1}, respectively. The mean PV for NO_x for ambient air was 0.016 cm s^{-1}, with a maximum PV of 0.038 cm s^{-1}. The PV's for formaldehyde and methanol were 0.018 cm s^{-1} and 0.026 cm s^{-1}, respectively. For NH_2Cl, the residence time was lower than previous experiments as a result of the smaller flow cell (as explained in the previous chapter); however, the PV was 0.045 cm s^{-1} for the TOTO tiles. In addition, seven concrete samples of varying concrete types and amounts of TiO_2 were tested. The highest PV from the concrete samples was 0.054 cm s^{-1}, which was produced by P25 concrete. Therefore, the highest overall photocatalytic reduction occurred with the reduction of NH_2Cl by the concrete sample.

A more important question regarding the tiles is the impact that they may potentially have on atmospheric chemistry through the removal of the studied pollutants. NO_x removal may lead to decreases in particulate matter (PM) concentrations by decreasing the amount of gas-phase HNO_3 that can potentially form PM. In addition, reducing NO_x can potentially lower ozone (an EPA criteria pollutant) which is formed through photochemical reactions involving volatile organic compounds (VOC's). In order to roughly assess the impact of surface reactions on TiO_2 impregnated tiles it is possible to use the deposition velocities (or PV's) estimated from the experiments, along with known ambient NO_x concentrations, to estimate the total removal rate of

NO_x due to photocatalytic reactions taking place on tile surfaces. The Georgia EPD reports a NO_x emissions inventory for Fulton County of 40,000 tons yr^{-1}. If we assume that the tiles are placed near emissions sources, that NO is being primarily emitted and the ambient concentration of NO is 60 μg m^{-3} (which is equivalent to 50 ppb that is roughly the annual mean value of NO_x for Fulton County, Georgia measured by the Georgia EPD) the total flux of NO using an upper PV value of 0.016 cm s^{-1} observed for the laboratory experiments over Fulton County is ~ 460 tons yr^{-1}. This estimate assumes that Fulton County has a surface area of 1385 km^2, and that this entire area is covered with tiles (which is of course not practical but the assumption is made to estimate how the tiles can potentially impact the ambient NO_x budget). The estimates do not take into account the lower deposition velocity of NO_2 to the tiles. It is worthwhile to note that other researchers have reported localized impacts of TiO_2 surfaces on NO_x (Maggos et al., 2007) and it should be pointed out that in situations where air is not well mixed with surrounding air containing NO_x it may be possible to achieve reductions on the order of several 10's of a percent.

In an indoor environment the TiO_2 tiles could improve the air quality. In a standard room the ventilation system completely recycles the air in one hour, or the air has a one hour residence time. If the TiO_2 tiles were placed into such a room the deposition of formaldehyde would be $1.6x10^{-4}$ μg m^{-3} s^{-1}, or 0.58 μg m^{-3} hr^{-1}. Although, an appropriate source of UV must shine on the tiles, a small surface coated with the TiO_2 would still remove a significant amount of formaldehyde.

Likewise, TiO_2 impregnated surfaces would reduce the exposure to monochloramine. The average concentration of NH_2Cl reported in pools is 0.1 mg/L, or 0.1 ppm (Li, 2009). This results in an ambient partial pressure of 0.87 ppm NH_2Cl, or 1.8 x 10^3 μg m^3. A standard swimming pool is approximately 25 meters long and 20 meters wide, and if we assume a 5 meter

perimeter of deck space that would equal 500 m^2 of deck. If the TiO_2 cement was placed into such a room the deposition of NH_2Cl would be 0.51 $\mu g\ m^{-3}\ s^{-1}$. If the cement covered the room and deck then the TiO_2 would remove 1.42 $mg\ s^{-1}$, or 5.07 $g\ hr^{-1}$. This might be slightly on the high side, considering that the dimensions of this room are large, but nonetheless there would be a significant reduction of gas phase monochloramine.

The natures of the tiles as well as the measurement techniques have some inherent limitations. The tiles can only oxidize pollutants at the tile surface, and yet most spaces of concern have a large volume. An increased residence time would overcome this problem. Experiments in the literature on chloramines report the gas phase reactions of NH_2Cl with HO^-, and other anionic nucleophiles, result in a nucleophilic substitution to form Cl^-. In addition, a competitive proton abstraction reaction forms $NHCl^-$ (Gareyev et al., 2001). This implies that additional unmonitored gas phase species might have formed. Alternatively, the UV photodecay of NH_2Cl in solution generates a series of radical reactions to produce NO_2^-, N_2O, NH_4^+, (Li and Blatchly, 2009). This suggests that N_2O and other species might have resulted after UV exposure, and may pose additional health threat. However, the true gas phase mass balance remains unknown. The PT-RMS can only detect molecules with a higher proton affinity than water, and N_2O which may have been generated, does not have a high enough proton affinity. In addition, the PT-RMS only distinguishes molecules by mass, and therefore two species with the same mass cannot be differentiated.

The photocatalytic reaction on the surface of TiO_2 results in the oxidation of a myriad of compounds. Future work will include a surface analysis that will determine additional byproducts of the chloramine reactions. X-ray photoelectron spectroscopy (XPS) analysis will resolve specific molecules formed on the tile surface. Additional work on the chloramine

compounds will determine the effect of di- and tri- chloramines on the tile surfaces. Alternative gas-phase techniques are needed to characterize all of the reaction products. Also, an alternative method then the one presented here is necessary to monitor trichloramine. This photocatalyst has universal appeal, and future work will undoubtedly discover more pertinent applications and underlying principles governing TiO_2 itself.

REFERENCES

Ao, C. H.; Lee, S. C.; Yu, J. Z.; Xu, J. H., Photodegradation of formaldehyde by photocatalyst TiO2: effects on the presences of NO, SO2 and VOCs. *Applied Catalysis B-Environmental* **2004,** *54* (1), 41-50.

Chen, F. N.; Yang, X. D.; Wu, Q., Antifungal capability of TiO2 coated film on moist wood. *Building and Environment* **2009,** *44* (5), 1088-1093.

Chen, J.; Ollis, D. F.; Rulkens, W. H.; Bruning, H., Photocatalyzed oxidation of alcohols and organochlorides in the presence of native TiO2 and metallized TiO2 suspensions. Part (II): Photocatalytic mechanisms. *Water Research* **1999,** *33* (3), 669-676.

Chong, M. N.; Jin, B.; Chow, C. W. K.; Saint, C., Recent developments in photocatalytic water treatment technology: A review. *Water Research* **2010,** *44* (10), 2997-3027.

Devahasdin, S., Fan, C., Li, K., Chen, D.H., TiO2 photocatalytic oxidation of nitric oxide: transient behavior and reaction kinetics, *J. Photochem. and Photobio., 156*, **2003**, 161-170.

Fang, S. C.; Cassidy, A.; Christiani, D. C., A Systematic Review of Occupational Exposure to Particulate Matter and Cardiovascular Disease. *International Journal of Environmental Research and Public Health* **2010,** *7* (4), 1773-1806.

Fujishima, A.; Hashimoto, K., Self cleaning and antibacterial effects of TiO2 containing and coated materials. *Abstracts of Papers of the American Chemical Society* **1996,** *211*, 263-PHYS.

Fujishima, A.; Honda, K., Electrochemical photolysis of water at a semiconductor electrode. *Nature* **1972,** *238* (5358), 37.

Gareyev, R.; Kato, S.; Bierbaum, V. M., Gas phase reactions of NH2Cl with anionic nucleophiles: Nucleophilic substitution at neutral nitrogen. *Journal of the American Society for Mass Spectrometry* **2001,** *12* (2), 139-143.

Hanson, D. R.; Greenberg, J.; Henry, B. E.; Kosciuch, E., Proton transfer reaction mass spectrometry at high drift tube pressure. *International Journal of Mass Spectrometry* **2003,** *223* (1-3), 507-518.

Heinsohn, R. J.; Kabel, R. L., *Sources and Control of Air Pollution*. Prentice-Hall, Inc.: Upper Saddle River, NJ, 1999.

Holzwarth, G.; Balmer, R.G.; Soni, L., The fate of chlorine and chloramines in cooling towers, *Wat. Res.*, **1984**, *18*, 1421-1427.

Jacobs, J. H.; Spaan, S.; van Rooy, G.; Meliefste, C.; Zaat, V. A. C.; Rooyackers, J. M.; Heederik, D., Exposure to trichloramine and respiratory symptoms in indoor swimming pool workers. *European Respiratory Journal* **2007,** *29* (4), 690-698.

Kawai, M.; Kawai, T.; Naito, S.; Tamaru, K., The mechanism of photocatalytic reaction over Pt/TiO2- production of H2 and aldehyde from gaseous alcohol and water. *Chemical Physics Letters* **1984,** *110* (1), 58-62.

Li, J.; Blatchley, E. R., Volatile disinfection byproduct formation resulting from chlorination of organic-nitrogen precursors in swimming pools. *Environmental Science & Technology* **2007,** *41* (19), 6732-6739.

Li, J.; Blatchley, E. R., UV Photodegradation of Inorganic Chloramines. *Environmental Science & Technology* **2009,** *43* (1), 60-65.

Lindinger, W.; Hirber, J.; Paretzke, H., An ion/molecule-reaction mass-spectrometer used for online trace gas-analysis. *International Journal of Mass Spectrometry and Ion Processes* **1993,** *129*, 79-88.

Linsebigler, A. L.; Lu, G. Q.; Yates, J. T., Photocatalysis on TiO2 surfaces- principles, mechanisms, and selected results. *Chemical Reviews* **1995,** *95* (3), 735-758.

Maggos, T., Bartzis, J.G., Leva, P., Kotzias, D., Application of photocatalytic technology for NOx removal, *Appl. Phys. A*, 89, 81-84, 2007a.

Maggos, T., Plassias, A., Bartzis, J.G., Vasilakos, C., Moussiopoulos, N., Bonafous, L., Photocatalyticdegradation of NOx in a pilot street canyon configuration using TiO2-mortar panels, Environ. Monit.Assess., DOI 10, 2007b.

Nemery, B.; Hoet, P. H. M.; Nowak, D., Indoor swimming pools, water chlorination and respiratory health. *European Respiratory Journal* **2002,** *19* (5), 790-793.

Noguchi, T.; Fujishima, A., Photocatalytic degradation of gaseous formaldehyde using TiO2 film. *Environmental Science & Technology* **1998,** *32* (23), 3831-3833.

Nowotny, J., Titanium dioxide-based semiconductors for solar-driven environmentally friendly applications: impact of point defects on performance. *Energy & Environmental Science* **2008,** *1* (5), 565-572.

Oberdorster, G., Pulmonary effects of inhaled ultrafine particles. *International Archives of Occupational and Environmental Health* **2001,** *74* (1), 1-8.

Oberdorster, G.; Ferin, J.; Finkelstein, G.; Wade, P.; Corson, N., Increased pulmonary toxicity of ultrafine particles. 2. Lung lavage studies. *Journal of Aerosol Science* **1990,** *21* (3), 384-387.

Pepi, F.; Ricci, A.; Rosi, M., Gas-phase chemistry of NHxCly+ ions. 3. Structure, stability, and reactivity of protonated trichloramine (vol 107A, pg 2088, 2003). *Journal of Physical Chemistry A* **2003,** *107* (31), 6121-6121.

Peral, J.; Ollis, D. F., Heterogeneous photocatalytic oxidation of gas-phase organics for air purification – acetone 1, butanol, butyraldehyde, formaldehyde, and meta-xylene oxidation *Journal of Catalysis* **1992,** *136* (2), 554-565.

Qi, H.; Sun, D. Z.; Chi, G. Q., Formaldehyde degradation by UV/TiO2/O-3 process using continuous flow mode. *Journal of Environmental Sciences-China* **2007,** *19* (9), 1136-1140.

Rioux, C. L.; Tucker, K. L.; Mwamburi, M.; Gute, D. M.; Cohen, S. A.; Brugge, D., Residential Traffic Exposure, Pulse Pressure, and C-reactive Protein: Consistency and Contrast among Exposure Characterization Methods. *Environmental Health Perspectives* **2010,** *118* (6), 803-811.

Salthammer, T.; Fuhrmann, F., Photocatalytic surface reactions on indoor wall paint. *Environmental Science & Technology* **2007,** *41* (18), 6573-6578.

Shang, C.; Gong, W. L.; Blatchley, E. R., Breakpoint chemistry and volatile byproduct formation resulting from chlorination of model organic-N compounds. *Environmental Science & Technology* **2000,** *34* (9), 1721-1728.

U.S. Environmental Protection Agency: An introduction to indoor air quality. http://www.epa.gov/iaq/formalde.html. Accessed: June 14, 2010.

Watanabe, T.; Nakajima, A.; Wang, R.; Minabe, M.; Koizumi, S.; Fujishima, A.; Hashimoto, K., Photocatalytic activity and photoinduced hydrophilicity of titanium dioxide coated glass. *Thin Solid Films* **1999,** *351* (1-2), 260-263.

Weaver, W. A.; Li, J.; Wen, Y. L.; Johnston, J.; Blatchley, M. R.; Blatchley, E. R., Volatile disinfection by-product analysis from chlorinated indoor swimming pools. *Water Research* **2009,** *43* (13), 3308-3318.

Zwiener, C.; Richardson, S. D.; De Marini, D. M.; Grummt, T.; Glauner, T.; Frimmel, F. H., Drowning in disinfection byproducts? Assessing swimming pool water. *Environmental Science & Technology* **2007,** *41* (2), 363-372.